Heliyon 6 (2020) e04778

Contents lists available at ScienceDirect

Heliyon

journal homepage: www.cell.com/heliyon

Research article

# Adaption of microbial communities to the hostile environment in the Doce River after the collapse of two iron ore tailing dams

Adriana Giongo [a,b,1], Luiz Gustavo dos Anjos Borges [a,1], Letícia Marconatto [a], Pâmela de Lara Palhano [a], Maria Pilar Serbent [b,c], Eduardo Moreira-Silva [a,d], Tiago de Abreu Siqueira [e], Caroline Thais Martinho [f], Rosalia Barili [f], Lisiê Valéria Paz [a,d], Letícia Isabela Moser [e], Carolina De Marco Veríssimo [g], João Marcelo Medina Ketzer [h], Renata Medina-Silva [a,d,*]

[a] Geobiology Laboratory, Instituto do Petróleo e dos Recursos Naturais (IPR), Pontifícia Universidade Católica do Rio Grande do Sul (PUCRS), Porto Alegre, Brazil
[b] Environmental Engineering Graduate Program, Universidade Regional de Blumenau (FURB), Blumenau, Brazil
[c] Sanitary Microbiology Laboratory, Department of Sanitary Engineering, Universidade do Estado de Santa Catarina (UDESC), Ibirama, Brazil
[d] Immunology and Microbiology Laboratory, School of Health and Life Sciences, Pontifícia Universidade Católica do Rio Grande do Sul (PUCRS), Porto Alegre, Brazil
[e] Geochemical Analyses Laboratory, Instituto do Petróleo e dos Recursos Naturais (IPR), Pontifícia Universidade Católica do Rio Grande do Sul (PUCRS), Porto Alegre, Brazil
[f] Sedimentology and Petrology Laboratory, Instituto do Petróleo e dos Recursos Naturais (IPR), Pontifícia Universidade Católica do Rio Grande do Sul (PUCRS), Porto Alegre, Brazil
[g] Laboratory of Parasite Biology, School of Health and Life Sciences, Pontifícia Universidade Católica do Rio Grande do Sul (PUCRS), Porto Alegre, Brazil
[h] Department of Biology and Environmental Sciences, Linnaeus University, Kalmar, Sweden

ARTICLE INFO

*Keywords:*
Aquatic ecology
Ecosystem change
Microbial ecology
Water pollution
Bacteria
Protozoa
Microbial genomics
Ore mining
Environmental impact
Metal tolerance
High throughput DNA sequencing

ABSTRACT

In November 2015, two iron ore tailing dams collapsed in the city of Mariana, Brazil. The dams' collapse generated a wave of approximately 50 million $m^3$ of a mixture of mining waste and water. It was a major environmental tragedy in Brazilian history, which damaged rivers, and cities 660 km away in the Doce River basin until it reached the ocean coast. Shortly after the incident, several reports informed that the concentration of metals in the water was above acceptable legal limits under Brazilian laws. Here the microbial communities in samples of water, mud, foam, and rhizosphere of *Eichhornia* from Doce River were analyzed for 16S and 18S rRNA-based amplicon sequencing, along with microbial isolation, chemical and mineralogical analyses. Samples were collected one month and thirteen months after the collapse. Prokaryotic communities from mud shifted drastically over time (33% Bray-Curtis similarity), while water samples were more similar (63% Bray-Curtis similarity) in the same period. After 12 months, mud samples remained with high levels of heavy metals and a reduction in the diversity of microeukaryotes was detected. Amoebozoans increased in mud samples, reaching 49% of microeukaryote abundance, with Discosea and Lobosa groups being the most abundant. The microbial communities' structure in mud samples changed adapting to the new environment condition. The characterization of microbial communities and metal-tolerant organisms from such impacted environments is essential for understanding the ecological consequences of massive anthropogenic impacts and strategies for the restoration of contaminated sites such as the Doce River.

## 1. Introduction

In November 2015, two iron ore waste dams collapsed in Mariana, Minas Gerais state, Brazil. The waste buried Bento Rodrigues sub-district with approximately 50 million $m^3$ of water and mining tailings (Escobar, 2015). The accident had a substantial impact on rivers and cities along the Doce River basin, reaching the marine environment 16 days later (IBAMA, 2015; Segura et al., 2016; Hatje et al., 2017). The Doce River's

* Corresponding author.
*E-mail address:* renata.medina@pucrs.br (R. Medina-Silva).
[1] These authors contributed equally to this work.

https://doi.org/10.1016/j.heliyon.2020.e04778
Received 14 February 2020; Received in revised form 25 May 2020; Accepted 20 August 2020

central basin is 83,400 km$^2$ wide and represents the primary water reservoir for 222 cities in Minas Gerais and Espírito Santo state (SAAE, 2015). The accident resulted in the deposition of a substantial load of suspended sediments and ore waste along the river basin. The subsequent increase in turbidity and chemical alteration of water caused the death of thousands of fish and other aquatic organisms along the river's 660 km and also affected many marine habitats (IBAMA, 2015; Fernandes et al., 2016; Miranda and Marques, 2016; Guerra et al., 2017; Gomes et al., 2018). The mining waste and water also spread over 1,775 ha of land along the river, including 835 ha of environmental protection areas, 236 ha of Atlantic Forest and 88 ha of natural vegetation (CONAMA, 2005; IBAMA, 2015; Miranda and Marques, 2016; SEDRU, 2016; SOS Mata Atlântica and INPE, 2016; Carmo et al., 2017). This disaster was rated as the most significant environmental tragedy in the country's history, and it is one of the largest tragedies involving mining activities in the world in the last century (IBAMA, 2015; Neves et al., 2016; Hatje et al., 2017).

In previous studies, chemical analyses performed on the muddy sediment and water collected at Governador Valadares or in different places along Doce River revealed high concentrations of heavy metals such as As, Cu, Fe, Hg, Mn, Zn, among others (SAAE, 2015; Segura et al., 2016; Hatje et al., 2017; Torres et al., 2017; Queiroz et al., 2018; Quadra et al., 2019). These elements are toxic to most organisms at specific concentrations (Amin, 2012).

Microbial characterization, along with chemical analyses, can help to assess the impact of anthropogenic activity on the natural environment. The disruption of natural bacterial community composition and, consequently, the establishment of a new microbial community with a specific metabolic potential necessary to inhabit tailings, have been demonstrated in studies evaluating environments impacted by the collapse of mining dams (Garris et al., 2018; Hatam et al., 2019). Several studies have already mentioned the eukaryotic ability to handle heavy metals in different contaminated environments. For example, protists have been found in highly stressful environments such as water bodies with extreme pH and temperature, low nutrients, and high levels of heavy metals (Zettler et al., 2002; Hu, 2014). The genus *Euglena*, former supergroup Excavata (Adl et al., 2019), has been well described in different surveys as metal tolerant in aquatic environments (Perales-Vela et al., 2006; Rehman, 2011; Płachno et al., 2015). Also, free-living amoebae (FLA) are an example of microeukaryote found in various environments under adverse conditions. FLA form cysts, which may remain for decades until they return to the active form (Sriram et al., 2008). FLA species isolated directly from impacted environments may adapt to higher concentrations of heavy metals than amoebae isolated from untouched environments (Amin, 2012).

Chemical analysis was carried out on the mud and water samples collected from the Doce River one and thirteen months after the collapse of the iron ore tailing dams. The similarity, diversity, and composition of the prokaryotic and microeukaryotic communities in mud, water, foam, and plant rhizosphere from this river were also compared.

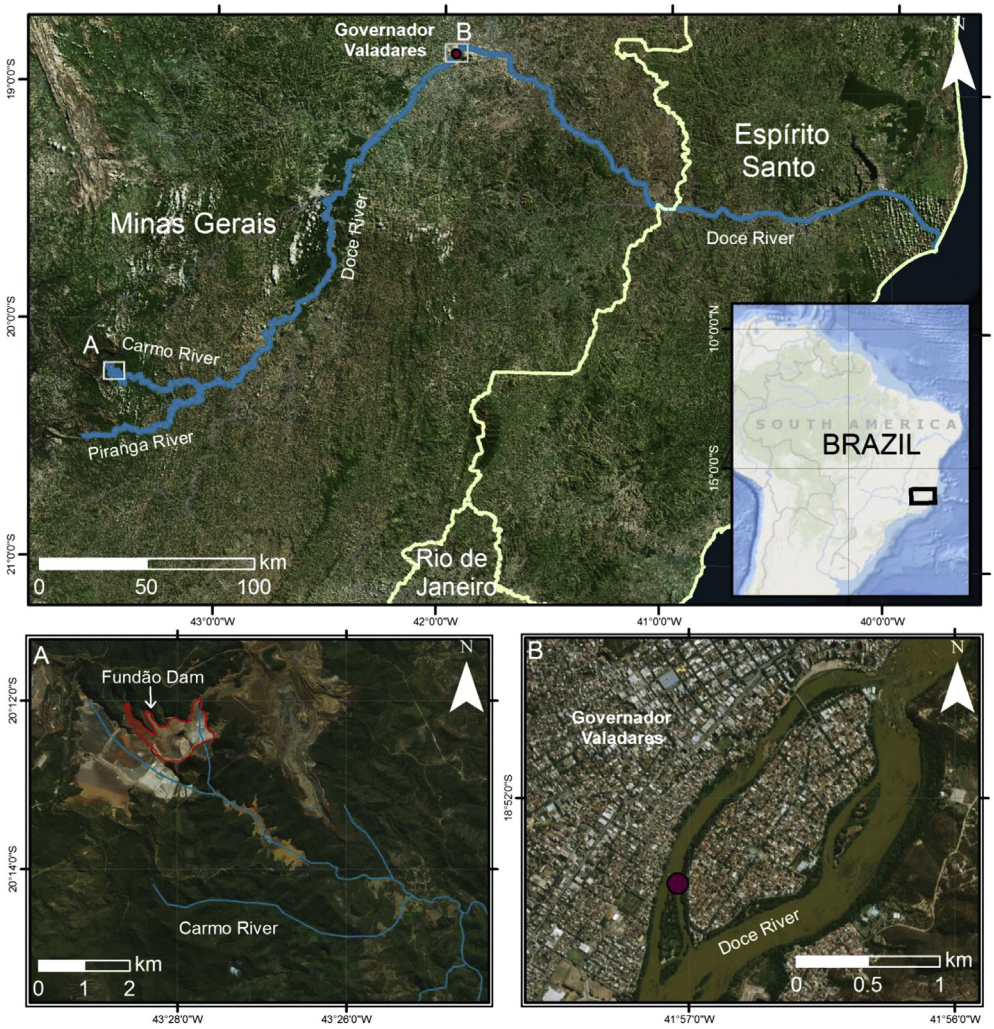


**Figure 1.** Map of Minas Gerais state and surrounding areas including the Doce River. (A) The local of the collapse of two iron ore tailing dams; (B) Aerial photographs of sampling site (red dot) in Governador Valadares, MG, around 250 km from the disaster area.

## 2. Material and methods

### 2.1. Origin and storage of samples

Samples were collected in two-time points at the Municipality of Governador Valadares (MG, Brazil) (Figure 1), approximately 250 km from the disaster area. The first sampling was conducted a month after the dam collapse (December 2015), in which water (W1) and mud sample (M1) were collected from Rio Doce. One year later, the second sampling of water (W13) and mud (M13) was carried out at the same geographic point. Additionally, samples of foam from the water surface (F13) and a sample from the rhizosphere of water hyacinth, *Eichhornia* (R13), which was blooming on the river, were also collected. As rhizosphere, we considered the soil tightly attached to the plant roots. All samples were collected aseptically, conditioned in 50 mL sterile plastic bottles at room temperature, and transported at 4 °C. Aliquots of water and mud samples were reserved to perform chemical and physicochemical analyses, while one aliquot of M1 sample was separated for bacterial cultivation. All others were stored at -80 °C.

### 2.2. Mineralogical analysis

Mineral identification was performed for mud samples following the procedures from Sedimentology and Petrology Laboratory (IPR/PUCRS) for XRD analysis of bulk and clay fraction samples. Sample M1 did not have volume enough to qualify for the analysis. For randomly oriented bulk sample analysis, 4 g of sediment M13 (a representative pool of replicates) were dried (60 °C for 12 h) and macerated using gral and pistil, avoiding the break of the mineral structures. This material was sifted through a 270 mesh and the undersized material was placed in a sample holder for powder bulk analysis, avoiding force the orientation of the mineral phases or press the sample in the holder. For XRD analysis of clay fraction, 8 g of dry bulk mixed with 150 mL of deionized water and 15 mL of sodium tetraphyro-phosphate were placed in an ultrasonic bath for 6 min for particles disaggregation. The sample was centrifuged at 750 rpm for 7 min. The supernatant was removed and then centrifuged for an additional 30 min at 3000 rpm. The settled material was smeared over a regular thin glass section for clay orientation. For this fraction, three treatments were applied before the analysis: (1) air-dried, (2) ethylene glycol saturated for 15 h (glycolate), and (3) heated at 490 °C in a muffle furnace for 5 h (calcination). The analysis was performed on a Bruker D8 Advance X-Ray Diffractometer with a Cu tube (40 kV and 30 mA). Randomly oriented bulk and air-dried oriented clay fractions were examined over the range of 3–70° 2θ with a step size of 0.015° 2θ and a count time of 0.2 s/step, while for the calcinate and glycolated samples, the range of 3–35° 2θ step size was used.

### 2.3. Chemical and physicochemical analyses

An inductively coupled plasma optical emission spectrometer (Perkin Elmer, Optima 7000 DV) was used to determine the metal content in samples M1, W1, M13, and W13 (the latter two in a representative pool of replicates). The metals analyzed in the mud and water samples were Ag, Al, Ba, Bi, Cd, Co, Cr, Cu, Fe, Li, Ni, and Pb. The calibration curve was performed in the range of 2.5 μg $L^{-1}$ to 1,000 μg $L^{-1}$, and the results were reported as the last reproductible value (quantification limit) to each metal analyzed.

M1 and M13 sediment samples were digested based on the EPA 3050B method (EPA, 2007). Approximately 0.4 g of dry sample was transferred to glass digestion tubes (100 mL), and 4 mL of concentrated nitric acid was added. The samples were digested in a heating block at 95 ± 5 °C for 15 min. After cooling, 2 mL of nitric acid was added, and heating continued at the same temperature for 30 min. Then, the samples were again cooled to the addition of 0.8 mL of ultrapure water (18.2 MΩ cm) and 1.2 mL of 30% hydrogen peroxide, and heated to 95 ± 5 °C for a further 2 h. Aliquots of hydrogen peroxide were added to the tubes until effervescence ceased, then 4 mL of concentrated hydrochloric acid was added, and the samples were heated for 15 min. Finally, the cold solutions were filtered and transferred to polypropylene vials and the volume made up to 50 mL with ultrapure water. All samples were filtered with 0.22 μm membranes and further analyzed in triplicates. Blank analyses were measured using ultrapure water. The procedures were conducted according to EPA (2007) methods. All observed values for the analyzed metals were compared, when applied, to the Brazilian legislation (CONAMA, 2005).

Physicochemical parameters were evaluated in triplicates for each water samples, except for sample W1, that presented solid particulates in amount that exceeded the limits acceptable by the methodologies applied. The pH analysis was performed according to ASTM E70-19 (ASTM, 2019) using the pH meter model DM-23 (Digimed Analytical Instrumentation). Conductivity was measured after meter standardization at 25°C ± 0.1 by a standard conductivity solution of 1413 μS $cm^{-1}$ using the meter of conductivity model DM-32 (Digimed Analytical Instrumentation). The conductivity was measured under temperature control and calculating the average value of triplicates (Eaton et al., 1998). The water color was measured by a visual comparison between ultrapure water and water sample using a water photometer (Aquacolor Cor, Policontrol) calibrated with standard ultrapure water. The samples were analyzed in triplicate at 25 °C ± 0.1 (CONAMA, 2005). The turbidity of the water was obtained through the nephelometric method using the turbidimeter model TD-300 (Instrutherm). The measures were based on comparing the intensity of light scattered by the contained static water sample to the intensity of light scattered by the reference standard in the sample container (ASTM, 2000).

### 2.4. Bacterial isolation, characterization and iron tolerance

Sample M1 was submitted to bacterial isolation in the presence of iron. A volume of 100 μL of mud was inoculated into 5 mL Luria Bertani (LB) broth (10 g $L^{-1}$ peptone; 5 g $L^{-1}$ yeast extract; 10 g $L^{-1}$ NaCl) supplemented with amphotericin B (2.5 μg $mL^{-1}$) and 1 mM Fe. Cultures were incubated under agitation at 100 rpm at 28 °C for up to 48 h, according to previous studies (Giovanella et al., 2016, 2017).

Bacterial cultures were diluted and plated on LB agar medium (1.5% agar) with 1 mM Fe and incubated at 28 °C until colonies appeared. Isolated bacterial colonies were purified and classified under optical microscopy (1,000 X) for their shape, arrangement, and also by Gram staining. Isolates were stored in 30% glycerol at -80 °C.

The test of tolerance to iron was performed inoculating the isolates into LB broth with three different concentrations of Fe (1 mM, 5 mM, 10 mM). The tubes were incubated at 28 °C for up to 48 h when they were observed for positive or negative microbial growth, which was detected by visual turbidity test of the bacteria cultures.

### 2.5. rRNA amplicon sequencing

Total DNA was extracted from 400 μL of water, 250 mg of mud, 400 μL of foam, and 400 μL of the washed rhizosphere, using DNeasy PowerSoil Kit (Qiagen) following the manufacturer's protocol. A 290-bp fragment from the V4 region of the 16S rRNA gene was amplified using the 515F and 806R universal archaeal and bacterial primers (Bates et al., 2011) and amplification was performed as described: 50-μL mixture consisting of 1.5 mM $MgCl_2$, 0.2 μM from each primer, 0.2 mM of each dNTP, 1U Platinum Taq DNA polymerase, 1X PCR reaction buffer, and 10 ng of genomic DNA. DNA fragments of the 18S rRNA gene V3 region were amplified using the pair of primers Fw and Rv described for eukaryotes by Nolte et al. (2010). PCRs were performed as previously described (Vieira et al., 2018). After purification of PCR amplicons using Agencount AMPure Beads (Beckman Coulter), library construction was performed as described in the Ion Plus Fragment Library from an initial amount of 100 ng of DNA. All samples were sequenced in a multiplexed PGM run using barcode sequences to identify each sample of the total

sequencing output. Sequencing was conducted on an Ion PGM System (Thermo Fisher) using an Ion 316 chip, following the manufacturer's instructions. The 16S and 18S ribosomal RNA amplicons were processed using QIIME v1.9 (Caporaso et al., 2010) as previously described (Vieira et al., 2018). The clusters were assembled using a minimum identity of 97%, and chimeras were removed using the RDP reference database (Cole et al., 2013). Taxonomic assignment for 16S and 18S rRNA amplicons was obtained for 97% of minimum similarity using Silva databases version 132 (Quast et al., 2013). The number of sequenced 16S and 18S rRNA amplicons generated and used in further analysis were summarized in Table 1. Sequencing results were deposited in the National Center for Biotechnology Information (NCBI) under BioProject PRJNA554843.

The nonmetric multidimensional scaling (NMDS) was used in a ordination plot to display the Bray-Curtis dissimilarity index for the relative abundance of taxa using Past3 software (Hammer et al., 2001). Alpha diversity metrics, Chao1 (species' richness), and Shannon (diversity) were calculated for each rarefied sample using the *phyloseq* R package (McMurdie and Holmes, 2013). One-way ANOVA with Tukey's post hoc test ($p < 0.05$) was applied for alpha diversity indexes using Past3 software (Hammer et al., 2001).

Macroeukaryotic groups Metazoa and Archaeplastida were not included in the dataset analysis. Amoebozoan sequences were filtered for further analysis, and the percentage calculated based on the total amoebozoan sequences from the samples. For Excavata, Fungi, and SAR, the percentage of each microorganism was calculated to express its abundance in relation to total OTUs of its own group.

The canonical correlation analysis (CCA) was performed to understand how the chemical variables aluminum and iron relates to the microbiome OTUs on different sampling environments. Permutation test with 100 repetitions was applied using Past3 software (Hammer et al., 2001). The Spearman rank correlation was performed to measure the degree of association between specific OTUs observed on samples and iron and aluminum concentration using Past3 software (Hammer et al., 2001).

### 2.6. Amoeba isolation and identification

A 5 mL aliquot of sample W13 was maintained for 24 h at room temperature in 10 mL of Page's amoeba saline (PAS) (Khan et al., 2001), and then centrifuged at 3000 rpm for 10 min. The pellet was seeded in the center of plates containing PAS and 1.5% agar, coated with inactivated *Escherichia coli* (ATCC 25922), penicillin G/streptomycin (5000 U $mL^{-1}$; GIBCO) and amphotericin B (12.5 μg $mL^{-1}$; INLAB). The plates were incubated at 37 °C. Observation of microbial development and morphology was verified under the optical microscope (400X) and successive inoculations were performed to obtain axenic cultures. The axenic cultures were washed with PAS and gently scraped to obtain cysts and trophozoites. The plate supernatant was placed in sterile tubes and centrifuged at 1500 rpm for 5 min; the supernatant was discarded and 2 mL of the Peptone Yeast Glucose liquid medium (PYG medium) was added to resuspend the pellet. Centrifugation and resuspension were repeated with the PYG medium. Cysts were classified by morphology under optical microscopy (400 X) (Visvesvara, 1991).

Scanning electron microscopy (SEM) analyses were also performed with axenic cultures. Cells were resuspended with 200 μL of PAS, a pellet was transferred to the wells of the culture plates containing polylysine-bathed glass coverslips and covered with PYG medium, and kept at room temperature. After verifying adhesion of trophozoites and cysts on the coverslips, the material was fixed with 2.5% glutaraldehyde and washed with phosphate buffer saline (PBS; Thermo Fisher). They were then dehydrated with increased acetone concentration (30–100%) and finally metalized with gold. Images were obtained from a secondary electron detector at 15 kV (Scanning Electron Microscopy, INSPECT-F50, FEI) at the Central Laboratory of Microscopy and Microanalysis (LabCEMM/PUCRS).

For molecular identification, amoebae were transferred to culture flasks containing PYG liquid medium, 40 μL $mL^{-1}$ penicillin/streptomycin, and 2 μL $mL^{-1}$ amphotericin B (kept at room temperature). Adhesion of amoebae to the flask was observed at inverted microscope, then the culture medium was discarded, and the amoebae cells were washed and recovered on 1 mL of saline solution. This material was centrifuged at 1500 rpm for 5 min and resuspended with 200 μL PYG liquid medium. Total amoebozoan DNA was isolated using MagMAX Total Nucleic Acid Isolation Kit (Thermo Fisher). The pair of primers JDP1 and JDP2 (Schroeder et al., 2001) was used to generate a 400-bp-long DNA fragment from the 18S rRNA gene fragment (V3 region) specific for the genus *Acanthamoeba*. The PCR's mixture was done as described above, and PCR's condition was performed as follows: initial step at 94 °C for 5 min; 30 cycles of 94 °C for 1 min, 58 °C for 1 min, 72 °C for 1 min; and final step of 72 °C for 5 min. The DNA fragment was purified and sequenced on an ABI 3500 capillary sequencer following the manufacturer's protocols.

Consensus sequence similarity analysis was performed using the Basic Local Alignment Search Tool (BLAST) to verify the identity and then aligned using the ClustalW tool incorporated in MEGA X (Kumar et al.,

**Table 1.** Overview of the number of sequences and operational taxonomic units (OTUs) from the Doce River samples.

| | | 2015 | | 2016 | | | | | | | | | | | | | Total |
|---|---|---|---|---|---|---|---|---|---|---|---|---|---|---|---|---|---|
| | | W1 | M1 | W13a | W13b | W13c | W13d | W13e | W13f | M13a | M13b | M13c | F13a | F13b | F13c | R13 | |
| 16S rRNA | Input sequences | 191835 | 84982 | 280350 | 172002 | 204979 | 104587 | 181687 | 112867 | 2753 | 1613 | n/a | 156332 | 88557 | 149236 | 245536 | 1977316 |
| | Input mean length | 210 | 208 | 196 | 201 | 202 | 203 | 195 | 202 | 199 | 203 | | 190 | 199 | 197 | 197 | |
| | Good sequences* | 158492 | 69298 | 244873 | 155153 | 185070 | 94781 | 156103 | 101756 | 2414 | 1446 | | 130989 | 78937 | 131325 | 213934 | 1724571 |
| | Good mean length | 239 | 239 | 215 | 216 | 217 | 217 | 217 | 217 | 218 | 219 | | 215 | 215 | 215 | 217 | |
| | Representative sequences** | 87341 | 31515 | 186074 | 111406 | 137501 | 70428 | 111035 | 75597 | 1242 | 718 | | 96723 | 59938 | 96681 | 135555 | 1201754 |
| | Representative OTUs** | 1833 | 1508 | 1934 | 1803 | 1726 | 1855 | 2101 | 2031 | 449 | 349 | | 2552 | 2053 | 2606 | 3452 | |
| 18S rRNA | Input sequences | n/a | 82808 | 82349 | 83364 | 74286 | 87070 | 78645 | 131953 | 75050 | 60566 | 108763 | 165959 | 168426 | 43344 | 194809 | 1437392 |
| | Input mean length | | 169 | 194 | 190 | 197 | 186 | 195 | 199 | 199 | 210 | 197 | 201 | 193 | 195 | 194 | |
| | Good sequences* | | 62339 | 72007 | 70643 | 66704 | 71907 | 68591 | 117878 | 66378 | 57759 | 95481 | 151356 | 144777 | 38110 | 170103 | 1254033 |
| | Good mean length | | 206 | 213 | 212 | 212 | 212 | 214 | 215 | 217 | 217 | 216 | 214 | 213 | 213 | 213 | |
| | Representative sequences** | | 52824 | 68088 | 65085 | 63136 | 65993 | 63944 | 110826 | 58734 | 55959 | 81461 | 142775 | 133340 | 35690 | 153158 | 1151013 |
| | Representative OTUs** | | 674 | 587 | 722 | 540 | 625 | 589 | 624 | 798 | 260 | 770 | 981 | 1041 | 681 | 1560 | |

* sequences with a minimum length of 100 bp and minimum Phred score of 20.
** representative sequences and OTUs after USEARCH.

2018). Phylogenetic analyses were performed using the Phylogeny tool on MEGA X with reference sequences obtained from the Genbank database. Phylogenetic trees were constructed using the maximum-likelihood method and the Tamura-Nei model (Tamura and Nei, 1993). Statistical significance was measured by 1,000 bootstrap repetitions.

## 3. Results

### 3.1. Chemical and sedimentological analyses

Changes in metal concentration between the two sampling times in water (W1/W13), and mud (M1/M13) are shown in Table 2. Analysis of water samples indicated that there were no changes in the concentration of metals, which, except by the Cd, were below the detection limit of the equipment, and therefore, below the standard levels reported by Brazilian law. However, in mud samples (M1) Al and Fe concentrations (40,000-fold) were much higher than the standard levels reported for Brazilian legislation. Also, high concentrations were observed for other metals, such as Ba (27,000-fold), Pb (3,500-fold), Cd (1,200-fold), Cr (600-fold), Ni, and Cu (400-fold). The concentration of Al, Ba, Cu, and Ni levels in the mud decreased, while Cd, Cr, and Fe concentrations increased over the one-year period.

The water sample's physicochemical parameters were analyzed and compared with the water quality parameters indicated by the Brazilian legislation (Table 3). The water was slightly acidic (pH 6.3), and turbidity was four times higher than the reference value reported by the Brazilian standard. Similarly, the color parameter showed a result of 13.3% higher than the reference value.

The mineralogy of samples did not present significant differences between bulk and clay fractions. The bulk sample results evidenced the presence of quartz, kaolinite, muscovite, hematite, and goethite, while clay fraction presented kaolinite, muscovite, hematite, and goethite (Figure 2). These last two minerals are related to iron ore tailing content but also to the iron rick rocks in the region (Silva et al., 2006).

### 3.2. Bacterial isolation and tolerance to iron

The presence of iron-tolerant bacteria on mud would suggests that a microbiome with resilient bacteria community may adapt and perhaps be helpful to remediate the impacted caused on the micro-environment. The mud sample collected a month after the dam collapse and submitted to bacterial cultivation resulted in three bacterial isolates (B1Fe, B2Fe, and B3Fe) tolerant to Fe at 5 mM and 10 mM. The morphological characterization of these metal tolerant isolates under optical microscopy after Gram staining showed two Gram-negative (bacilli and coccobacilli) and one Gram-positive (cocci). It was also observed that the isolates inoculated in LB broth with Fe at 5 mM and 10 mM changed color from light yellow to green after 24 h of incubation.

### 3.3. Diversity of prokaryotic and eukaryotic communities

Bacterial taxonomic abundances were used to calculate a Bray-Curtis dissimilarity matrix of water and mud samples. Results were plotted in a two-dimensional NMDS plot (Figure 3A). The prokaryotic communities of water, along with foam and rhizosphere samples, were more similar to each other, clearly diverging from those of mud samples over time ($R^2 = 0.5406$; stress = 0.1435). The similarity between M1 and M13 samples was lower than the similarity between W1 and W13 samples (33% and 63%, respectively). The microeukaryotic communities from water, foam, and mud grouped separately from each other, except by the M1 sample, that was more similar to foam samples than to the M13 samples ($R^2 = 0.3709$; stress = 0.1152) (Figure 3B).

The most diverse and rich sample from the Doce River was the rhizosphere, for both prokaryote and eukaryote communities (Figures 3C, 3D). The prokaryotic diversity on mud is higher than the one observed on water ($p = 0.017$), and lower than the one observed in foam ($p = 0.023$) (Figure 3C). Regards to the richness, samples presented no significant differences among water, foam, and mud samples ($p = 0.671$). In contrast, microeukaryotes presented higher diversity on water than mud ($p = 0.004$) and foam ($p = 0.005$) samples (Figure 3D). As well as observed in the prokaryotic communities, a similar richness was observed among samples ($p = 0.303$).

### 3.4. Composition of microbial communities

A total of 796 ranked OTUs were assigned to 53 prokaryotic phyla (or candidate divisions). Acidobacteria, Actinobacteria, Bacteroidetes, Chloroflexi, Crenarchaeota, Firmicutes, Gemmatimonadetes, Nitrospirae, Proteobacteria, Verrucomicrobia and the candidate phyla "Gracilibacteria" (GN02) and "Latescibacteria" (WS3) (Rinke et al., 2013) were the ones with abundance higher than 1% of the total reads (Figure 4A). The dominating phylum in all samples was Proteobacteria, with an average of 70.8%. The second and third most abundant phyla in water samples were Actinobacteria and Bacteroidetes, with an average of 13.1% and 5.3% of sequences, respectively. The second and third most abundant phyla in the mud samples were Bacteroidetes and Actinobacteria (17% and 8.6% of the total sequences, respectively) in sample M1, and Nitrospirae and Acidobacteria (average 12.1% and 8.5% of the total sequences, respectively) in samples M13 (Figure 4A).

At the family level, forty-five OTUs presented an abundance higher than 1% of the total sequences (Figure 5). *Comamonadaceae* was the most abundant prokaryotic family in all samples (average of 21.5%), with higher abundances found in foam samples (average of 38.5%). Secondly, the family *Moraxellaceae* presented an average of 13.4% in W13 samples and 20.7% in the rhizosphere. The most abundant OTU in all samples (except R13) belongs to the family *Comamonadaceae*, with an average of 21.5% of the total sequences (minimum average of 11.6% in M13 and a maximum of 38.5% in F13 samples). In R13, the most abundant OTU

**Table 2.** Chemical analysis of metals found in water and mud samples collected from Doce River one month (M1 and W1) and 13 months (M13 and W13) after the dams' collapse. Procedures were conducted in triplicate according to EPA (2007) methods for each sample and compared with reference values of Brazilian legislation.

| Sample | Ag | Al | Ba | Bi | Cd | Co | Cr | Cu | Fe | Li | Ni | Pb |
|---|---|---|---|---|---|---|---|---|---|---|---|---|
| | mg.L-1 | | | | | | | | | | | |
| W1 | <0.007 | 0.037 ± 0.01 | 0.02 ± 0.00 | <0.47 | <0.011 | <0.0003 | <0.039 | <0.002 | 0.05 ± 0.01 | <0.0001 | 0.02 | <0.013 |
| W13* | <0.007 | <0.004 | 0.04 ± 0.01 | <0.47 | <0.011 | <0.0003 | <0.039 | <0.002 | <0.004 0.3 | <0.0001 | 0.02 | <0.013 |
| BL** | 0.01 | 0.10 | 0.70 | *** | 0.001 | 0.05 | 0.05 | 0.009 | 0.30 | 2.500 | 0.025 | 0.01 |
| | mg.kg-1 | | | | | | | | | | | |
| M1 | <2.10 | 4162.92 ± 637.33 | 19.40 ± 3.37 | <267.40 | 1.24 ± 0.22 | <0.42 | 34.31 ± 3.72 | 3.83 ± 0.13 | 12224.74 ± 707.99 | <0.09 | 9.06 ± 1.84 | <35.35 |
| M13* | <2.10 | 2227.75 ± 97.50 | 12.97 ± 2.88 | <267.40 | 2.07 ± 0.13 | <0.42 | 38.87 ± 1.01 | 3.43 ± 0.66 | 17534.75 ± 845.59 | <0.09 | 7.05 ± 1.06 | <35.35 |

* pool of biological replicates.
** Standard values for the Brazilian legislation (CONAMA, 2005).
*** Reference values not predicted in Brazilian legislation.

**Table 3.** Physicochemical parameters of water quality measured in the Doce River sample W13 compared with reference values of Brazilian legislation.

| Sample | T (°C) | pH | EC (μS cm-1) | Color (μC) | Turbidity (NTU) |
|---|---|---|---|---|---|
| W13 | 23.4 | 6.3 | 32.96 | 85.5 | 411 |
| BL* | ** | 6–9 | ** | ≤75 | ≤100 |

* Standard values for the Brazilian legislation (CONAMA, 2005).
** Reference values not predicted in Brazilian legislation.

belongs to the family *Moraxellaceae*, representing 17.8% of the total sequences; the same OTU was the second most abundant in W13 samples (average 11%) (Table 4). Samples W1 and W13 also presented a high abundance of Actinomycetales ACK-M1 (7.4% and 10.5% of the total sequences, respectively), a typical OTU from most freshwater habitats (Van der Gucht et al., 2005). *Flavisolibacter*, belonging to the family *Chitinophagaceae*, was the second most abundant prokaryotic microorganism in the M1 sample, representing more than 10% of the total sequences.

Five main groups of microeukaryotes were identified based on the classification of eukaryotes described by Adl et al. (2012). Amoebozoa, Cryptophyceae, Excavata, Opisthokonta (subdivided among Fungi and Holozoa), and SAR (subdivided in Alveolata, Rhizaria, and Stramenopiles) presented high abundance in all samples (Figure 4B). Alveolata and Stramenopiles dominated the water and rhizosphere samples, while Fungi was more abundant in foam and mud samples. Amoebozoa strongly dominated the microenvironment of mud samples M13 (>49.9% of the total sequences).

Kinetoplastea was the most abundant Excavata class, with abundance ranging from 51% of the Excavata sequences in M1 to 93.9% (average) in F13 samples. The genus *Neobodo* dominated the F13 sample (more than 77.1% of the total Excavata sequences), and along with the genus *Bodo*, also dominated the samples R13, M1 and M13 (average 22.2%). More than half of the Excavata sequences in W13 belonged to an OTU belonging to the Order Trypanosomatida (Table 5). Among the Fungi, an unclassified OTU belonging to the phylum Mucoromycota was the most abundant fungi in M13 samples, with an average of 56.6% of the fungal sequences. In M1, R13 and F13 samples, an unclassified OTU belonging to the family *Phaeosphaeriaceae* dominated the sequences, while in W13, an OTU from the order Agaricales was the most abundant fungi in that samples.

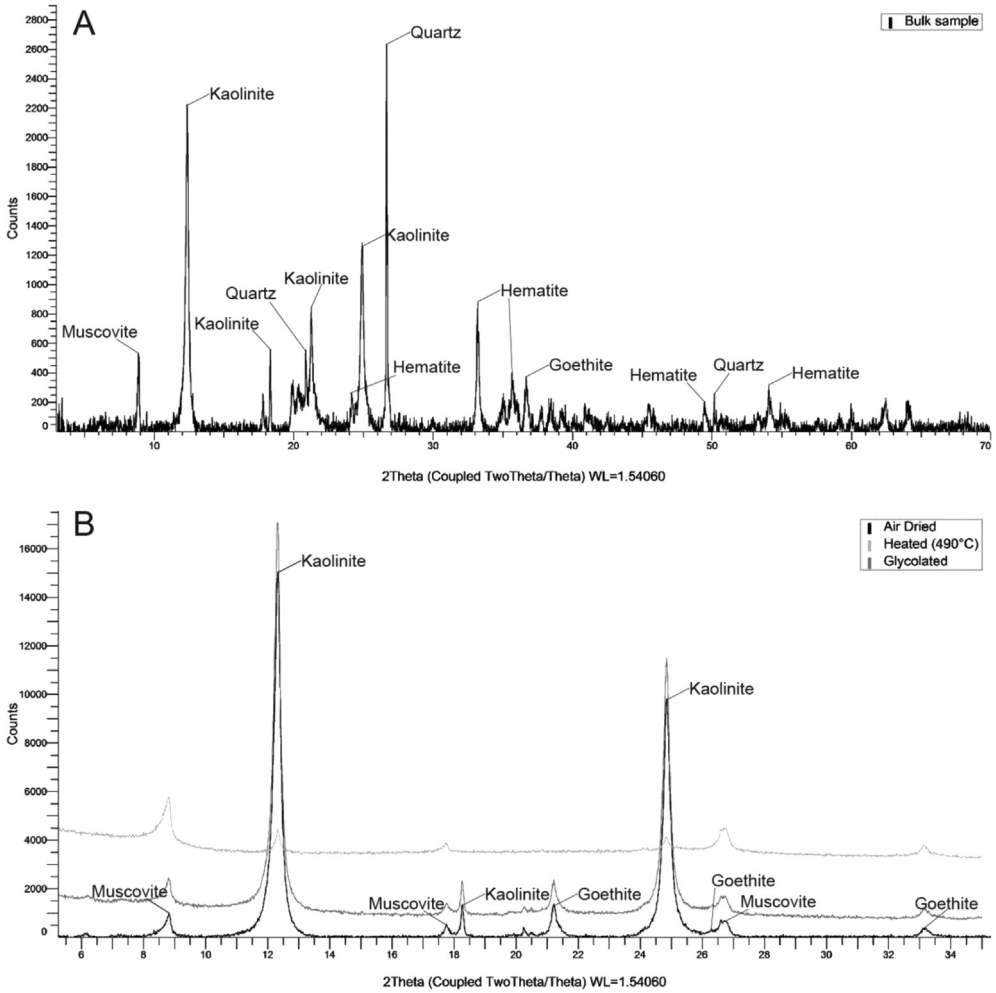


**Figure 2.** XRD analysis from drained sediment from Doce River. (A) Bulk sample; (B) Oriented clay fraction. Mineralogy is indicated in A and B and sample treatment (for oriented clay) is indicated in B. The analysis was performed on a Bruker D8 Advance X-Ray Diffractometer with Cu tube (40 kV and 30 mA) following the procedures from Sedimentology and Petrology Laboratory (IPR/PUCRS).

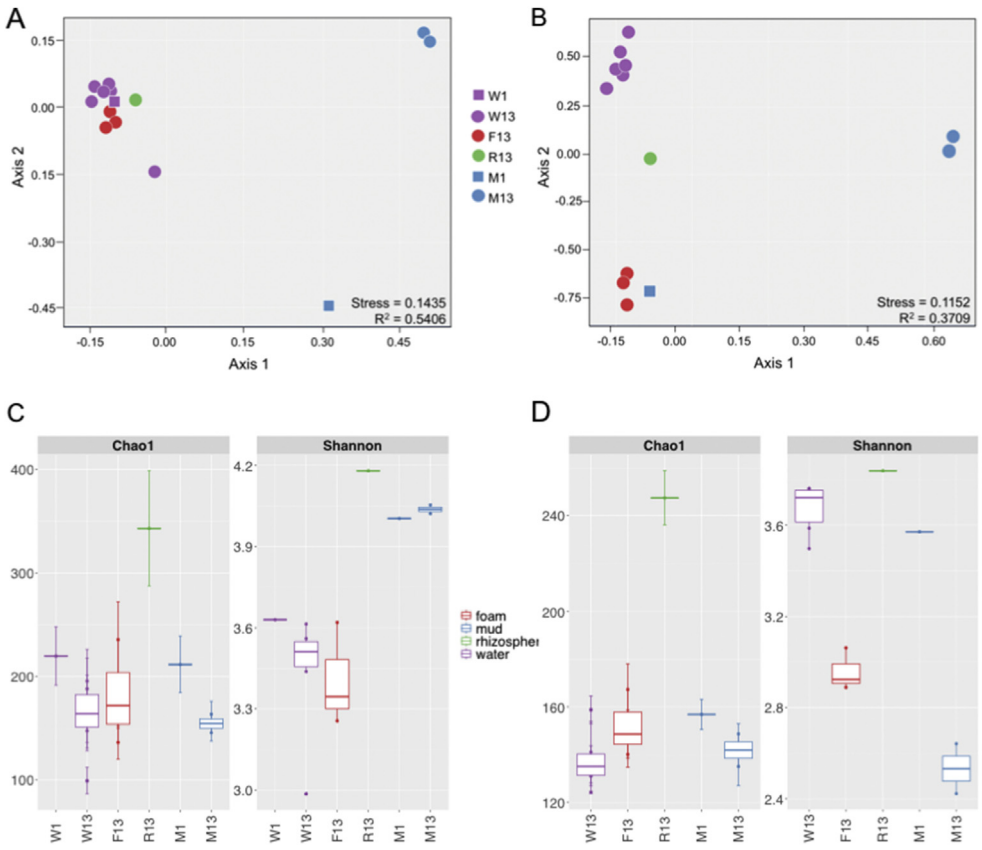


**Figure 3.** NMDS and alpha diversities from microbial communities. Non-metric multidimensional scaling (NMDS) ordinations of Bray-Curtis dissimilarity matrix of (A) the prokaryotic; and (B) microeukaryotic communities from samples from the first and thirteenth months after the disaster. Alpha diversity measured by Chao1 (species' richness) and Shannon (diversity) indexes for (C) prokaryotes; and (D) microeukaryotes. One-way ANOVA with Tukey's post-hoc test was used ($p < 0.05$).

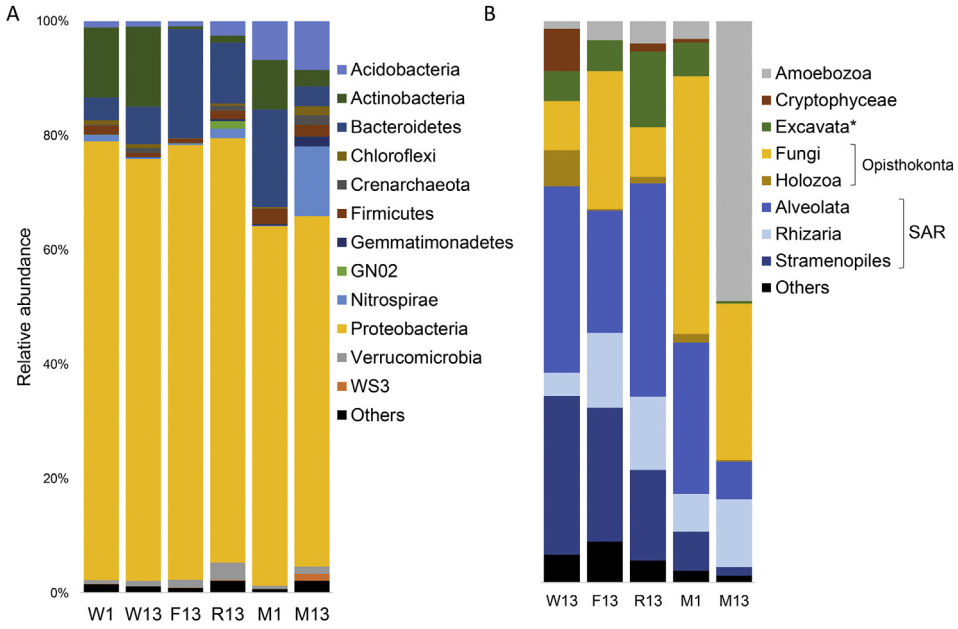


**Figure 4.** Microbial profile of the Doce River samples. (A) most abundant prokaryotic phyla; and (B) main microeukaryotic supergroups. Others corresponds to groups with abundance lower than 1% of the total sequences.

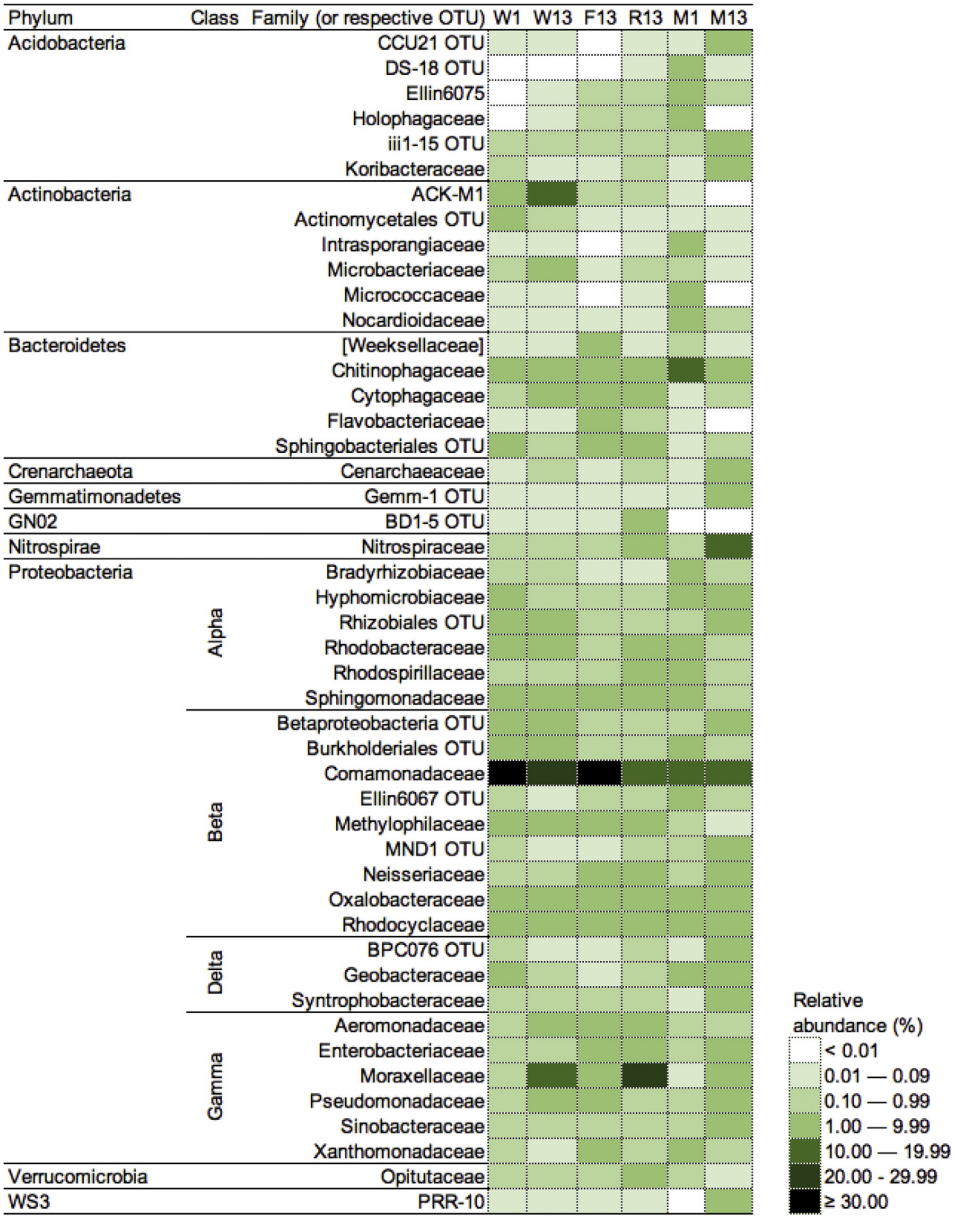


**Figure 5.** Heatmap of the most frequent prokaryotic families (or correspondent OTU) based on the 16S rRNA amplicon sequencing.

The Alveolata genus *Hypotrichia* was the most abundant SAR organism in W13 samples (11% of the SAR sequences), while the genus *Cyrtophoria*, also from Alveolata, was the dominant SAR in F13 and M1, representing 24.4% and 18.9% of the total SAR sequences. In R13, *Blepharisma* (Alveolata) represented almost 44% of the SAR sequences in the rhizosphere sample. In M13, an OTU belonging to the Euglyphida (Rhizaria) dominated in samples M13.

### 3.5. Amoebozoa identification

The 18S rRNA sequencing identified a total of 33 OTUs classified as belonging to the Supergroup Amoebozoa. The amoebozoan groups Discosea, Gracilipodida, and Tubulinea were present in all samples, although in different proportions (Figure 6A). Discosea was the most abundant group in all samples (average 61.6% of the amoebozoan sequences), except by M1 (average 13.7%). In M1, Gracilipodida was the most abundant, followed by Tubulinea and Discosea, which presented each an average of 14% of the total amoebozoan sequences each. The seventeenth most abundant amoebozoans were summarized in Figure 6B.

*Flamella* was the most abundant genus in the M1 sample, followed by *Acanthamoeba, with 32.6% and 10.8% of the total amoebozoan sequences, respectively*. *Acanthamoeba* was the most abundant genus in W13 and M13 samples, with an average of 33% and 80% of the Amoebozoa sequences, respectively. In F13 samples, an unclassified Euamoebida OTU was the most abundant amoebozoan, followed by the genus *Acanthamoeba* (45.5% and 28% of the total amoebozoan sequences, respectively).

Phylogenetic analysis based on a 400-bp segment of the 18S rRNA V4 region demonstrated that the isolated amoeba from sample W13 was placed within a clade containing the species *Acanthamoeba lenticulata* (Figure 6C). The morphological analysis of the amoeba culture under optical microscopy (400 X) indicated that the amoeba presented typical

**Table 4.** Most abundant prokaryotic genera (or correspondent OTUs) across Doce River samples obtained by 16S rRNA amplicon sequencing. "Others" combine the OTUs with abundance lower than 1% of the total prokaryotic sequences.

| Phylum | Class | Order | Family | Genus | Relative abundance (%) | | | | | |
|---|---|---|---|---|---|---|---|---|---|---|
| | | | | | W1 | W13 | F13 | R13 | M1 | M13 |
| Acidobacteria | [Chloracidobacteria] | RB41 | Ellin6075 OTU | | 0 | 0.03 | 0.10 | 0.33 | 2.79 | 0.49 |
| | Acidobacteria-6 | Pirellules | CCU21 OTU | | 0.02 | 0.01 | 0.004 | 0.06 | 0.03 | 1.33 |
| | | | iii1-15 OTU | | 0.31 | 0.35 | 0.24 | 0.37 | 0.28 | 2.00 |
| | Acidobacteriia | Acidobacteriales | Koribacteraceae OTU | | 0.05 | 0.01 | 0.003 | 0.10 | 0 | 1.33 |
| | Holophagae | Holophagales | Holophagaceae | *Geothrix* | 0.005 | 0.01 | 0.07 | 0.09 | 1.09 | 0 |
| | iii1-8 | DS-18 OTU | | | 0 | 0.0004 | 0.001 | 0.01 | 1.07 | 0.07 |
| Actinobacteria | Actinobacteria | Actinomycetales | ACK-M1 OTU | | 7.36 | 10.46 | 0.10 | 0.37 | 0.03 | 0 |
| | | | Microbacteriaceae OTU | | 0.26 | 1.24 | 0.03 | 0.09 | 0.11 | 0.07 |
| | | | Micrococcaceae OTU | | 0.03 | 0.003 | 0.003 | 0.02 | 2.93 | 0 |
| | | | Nocardioidaceae OTU | | 0.09 | 0.01 | 0.03 | 0.05 | 2.18 | 0.29 |
| | | Actinomycetales OTU | | | 1.45 | 0.81 | 0.03 | 0.07 | 0.04 | 0.15 |
| Bacteroidetes | [Saprospirae] | [Saprospirales] | Chitinophagaceae | *Flavisolibacter* | 0.005 | 0.01 | 0.07 | 0.07 | 10.68 | 0 |
| | | | | *Sediminibacterium* | 0.35 | 1.72 | 3.11 | 0.88 | 0.40 | 0 |
| | | | Chitinophagaceae OTU | | 0.99 | 0.91 | 3.58 | 2.69 | 4.01 | 1.64 |
| | Cytophagia | Cytophagales | Cytophagaceae | *Flectobacillus* | 0 | 0.07 | 2.83 | 0.29 | 0.12 | 0 |
| | | | Cytophagaceae OTU | | 0.19 | 1.78 | 0.12 | 2.05 | 0.41 | 0.11 |
| | Flavobacteriia | Flavobacteriales | Flavobacteriaceae | *Flavobacterium* | 0.01 | 0.03 | 2.82 | 0.12 | 0.01 | 0 |
| | | | [Weeksellaceae] | *Cloacibacterium* | 0.01 | 0.06 | 2.41 | 0.08 | 0.11 | 0 |
| | Sphingobacteriia | Sphingobacteriales OTU | | | 1.53 | 0.98 | 1.06 | 1.93 | 0.23 | 0.68 |
| Crenarchaeota | Thaumarchaeota | Cenarchaeales | Cenarchaeaceae OTU | | 0.09 | 0.73 | 0.01 | 0.60 | 0.01 | 1.41 |
| Gemmatimonadetes | Gemm-1 OTU | | | | 0.01 | 0.01 | 0.01 | 0.08 | 0.03 | 1.70 |
| GN02 | BD1-5 OTU | | | | 0.05 | 0.05 | 0.04 | 1.33 | 0.003 | 0 |
| Nitrospirae | Nitrospira | Nitrospirales | Nitrospiraceae | *Nitrospira* | 0.67 | 0.17 | 0.25 | 1.53 | 0.15 | 10.29 |
| Proteobacteria | Alphaproteobacteria | Rhizobiales | Bradyrhizobiaceae | *Balneimonas* | 0.01 | 0.003 | 0.002 | 0.01 | 2.01 | 0 |
| | | | Hyphomicrobiaceae | *Hyphomicrobium* | 0.28 | 0.06 | 0.04 | 0.09 | 0.28 | 1.73 |
| | | Rhizobiales OTU | | | 3.35 | 1.36 | 0.18 | 0.39 | 0.73 | 2.18 |
| | | Rhodobacterales | Rhodobacteraceae | *Rhodobacter* | 2.02 | 1.98 | 0.44 | 0.64 | 0.42 | 0 |
| | | Rhodospirillales | Rhodospirillaceae | *Azospirillum* | 0.04 | 0.02 | 0.01 | 1.20 | 0.12 | 0 |
| | | Sphingomonadales | Sphingomonadaceae | *Kaistobacter* | 0.10 | 0.03 | 0.24 | 0.17 | 3.67 | 0.08 |
| | | | | *Novosphingobium* | 0.76 | 0.47 | 2.72 | 1.99 | 1.40 | 0.11 |
| | | | | *Sphingomonas* | 0.08 | 0.01 | 0.20 | 0.15 | 1.25 | 0.07 |
| | | | Sphingomonadaceae OTU | | 1.62 | 0.68 | 0.53 | 0.36 | 0.56 | 0.18 |
| | Betaproteobacteria | Burkholderiales | Comamonadaceae | *Comamonas* | 3.47 | 0.06 | 0.43 | 0.11 | 0.35 | 0 |
| | | | | *Hydrogenophaga* | 0.92 | 3.00 | 1.69 | 2.08 | 1.79 | 0.16 |
| | | | Comamonadaceae OTU | | 29.79 | 24.56 | 38.49 | 12.12 | 12.36 | 11.56 |
| | | | Oxalobacteraceae | *Polynucleobacter* | 4.98 | 3.09 | 0.34 | 0.15 | 0.32 | 0 |
| | | | Oxalobacteraceae OTU | | 3.05 | 1.31 | 2.20 | 2.10 | 7.17 | 1.72 |
| | | Burkholderiales OTU | | | 1.47 | 3.23 | 0.57 | 0.38 | 1.12 | 0.14 |
| | | Ellin6067 OTU | | | 0.10 | 0.08 | 0.21 | 0.42 | 2.05 | 0.69 |
| | | Methylophilales | Methylophilaceae OTU | | 2.51 | 1.89 | 0.71 | 0.85 | 0.20 | 0.04 |
| | | MND1 OTU | | | 0.19 | 0.08 | 0.07 | 0.39 | 0.11 | 1.28 |
| | | Neisseriales | Neisseriaceae | *Vogesella* | 0.07 | 0.18 | 0.93 | 2.29 | 0.40 | 0.43 |
| | | | Neisseriaceae OTU | | 0.001 | 0.05 | 0.25 | 1.65 | 0 | 0 |
| | | Rhodocyclales | Rhodocyclaceae | *Azospira* | 0.04 | 0.01 | 0.02 | 0.14 | 1.96 | 0.04 |
| | | | | *Dechloromonas* | 0.29 | 0.27 | 0.32 | 1.57 | 2.22 | 0.57 |
| | | | Rhodocyclaceae OTU | | 3.69 | 0.75 | 0.41 | 2.19 | 4.09 | 3.79 |
| | Betaproteobacteria OTU | | | | 1.55 | 2.11 | 0.43 | 0.89 | 0.63 | 2.82 |
| | Deltaproteobacteria | BPC076 OTU | | | 0.37 | 0.08 | 0.01 | 0.14 | 0.01 | 1.56 |
| | | Desulfuromonadales | Geobacteraceae | *Geobacter* | 1.21 | 0.09 | 0.08 | 0.80 | 1.90 | 1.03 |
| | | Syntrophobacterales | Syntrophobacteraceae OTU | | 0.31 | 0.18 | 0.13 | 0.19 | 0.02 | 3.38 |
| | Gammaproteobacteria | Aeromonadales | Aeromonadaceae OTU | | 0.14 | 0.90 | 1.53 | 1.33 | 0.34 | 0.85 |
| | | Enterobacteriales | Enterobacteriaceae OTU | | 0.81 | 0.76 | 2.55 | 0.86 | 0.24 | 3.95 |
| | | Pseudomonadales | Moraxellaceae | *Acinetobacter* | 0.17 | 2.28 | 2.71 | 2.37 | 0.04 | 0.65 |
| | | | Moraxellaceae OTU | | 0.15 | 11.03 | 2.52 | 17.79 | 0.02 | 1.29 |
| | | Pseudomonadales | Pseudomonadaceae | *Pseudomonas* | 0.34 | 3.33 | 1.38 | 0.85 | 0.37 | 5.04 |
| | | Xanthomonadales | Sinobacteraceae OTU | | 0.51 | 0.58 | 0.55 | 0.40 | 0.15 | 1.43 |
| | | | Xanthomonadaceae | *Lysobacter* | 0.01 | 0.001 | 0.03 | 0.004 | 2.13 | 0 |
| WS3 | PRR-12 | Sediment-1 | PRR-10 OTU | | 0.07 | 0.02 | 0.01 | 0.08 | 0.003 | 1.15 |

characteristics of the genus *Acanthamoeba* (Visvesvara, 1991). This information was confirmed under SEM analysis, in which individual amoebas were observed in detail (to maximum 20.000 X) (Figure 6D).

### 3.6. Chemical and microbiome correlation

We performed CCA to infer the influence of the variability observed of iron and aluminum levels on the microbial communities (Figure 7). A high abundance of amoeba OTUs, specially *Ischnamoeba*, *Acanthamoeba*, and OTUs belonging to the group Centramoebida and BOLA868 (group I) are very likely to be found where iron concentration is increased. The association of high concentrations of iron in mud samples and the abundance of those OTUs was explained by 56% of the analyzed variable. On the other side, a group of prokaryotes, mainly the genera *Balneimonas*, *Lysobacter*, *Azospira*, *Kaistobacter*, and *Sphingomonas* (Proteobacteria), *Flavisolibacter* (Bacteroidetes), and *Geothrix* (Acidobacteria), along with the amoebozoan genus *Flamella* (group II), seemed to be more associated to higher levels of aluminum. The high abundance over samples observed for sequences belonging to the family *Comamonadaceae*, including the genera *Hydrogenophaga* and *Comamonas*, presented no specific correlation with one of those chemical variables tested (iron or aluminum). Permutation test performed demonstrated significance on both correlations analyzed ($p = 0.01961$).

## 4. Discussion

The recovery time required for environments that pass through catastrophic events is dependent on the combined effort made by the government and local communities. That recovery can be monitored through the variations observed, among a range of biotic and abiotic parameters, in the microenvironment. Our study has described the microbial community on Doce River right after receiving a massive amount of mining waste and water, the consequence of a major environmental tragedy.

The microbial analysis revealed two main microbial clusters defined by water and mud samples. Into the water cluster, samples were moderately similar (63% similarity) over time. Since the first month after the Doce River waters received the mining waste, it seems that an exogenous microbiota has been harbored by the river and has not changed quickly enough. Possibly, the steady physicochemical changes, such as high-water turbidity, have been responsible for the slow changes on the microbial profile. Comparatively, prokaryotic communities showed 33% of similarity into mud samples M1 and M13. In this case, chemical changes, such as the concentration of heavy metals observed since the first month after the dam collapse, might have been the most important environmental factor of the selection of prokaryotic taxa over time.

The high turbidity of water after the dam collapse may have contributed to the high abundance of microorganisms since particulates also provide habitats for aerobic and anaerobic communities (Xia et al., 2014). Sediment clays found in mud, such as goethite, can contribute to water turbidity, as well as organic and non-crystalline compounds. Moreover, hematite and goethite are related to iron ore tailings content, but also the iron-rich rocks in the study region (Silva et al., 2006). Savio et al. (2015) reported that the presence of heterogeneous particles in water provides an increase in niche availability in river samples. Furthermore, while the levels of iron and other heavy metals in water were below thresholds since the first month after the disaster, the mud samples had high amounts of heavy metals along all this period. This behavior may be related to the high ore density (Silva et al., 2017) that propitiate the particle settling, and to the solute adsorption potential of the clay minerals due to its large specific surface area and surface charge (Yuan et al., 2013). However, the observed mineralogy for the collected samples does not indicate expansible clays such as montmorillonite.

In contrast to water, mud samples had high concentration of Fe and other heavy metals like Al, Ba, Cd, Cr, Cu, Ni, and Pb, since the first month of sampling. When oxidized in an aquatic system, Fe is converted to ferric hydroxide that is quickly precipitated and deposited (Hem and Cropper, 1959). Each element has a different solubilization rate, affecting dissolution, suspension and sedimentation of the metals in different levels. It might explain the increase or decrease of each analyzed metal in the mud over the sampling period. Since metals are deposited in sediments after adsorbed into organic and inorganic particulates, mud, like other sediments, has been recognized as a secondary source of pollution of water (Liu et al., 2008; Pobi et al., 2019).

Heavy metals alter the natural microbial communities of sediment and soil, possibly leading to the loss of bacterial species responsible for nutrient cycling (Piotrowska-Seget et al., 2005; Chen et al., 2018). Therefore, contrary to our expectations, prokaryotic diversity did not decrease in the heavy metal-contaminated mud after 12 months. However, the reduction on richness of species indicates that some species were favored in an adaptation process to the newly established environment. While the high concentration of heavy metals in the mud sediment (M1 and M13) may not have a direct impact on prokaryotic diversity, NMDS with Bray-Curtis analysis suggest that changes in microbial composition occurred from the first to the thirteenth month after the collapse.

We may consider that the ore waste in Doce River water may have promoted niches and nutrient sources that were not present in the environment in the past. Although microbial communities present sensitiveness to metal pollution, when endangered by long-term exposure to metal leads, they can show resistance, tolerance, or resilience (Azarbad et al., 2016). We have identified several bacterial groups described as tolerant in stressful environments. Some of them seem to be microenvironment dependent, such as Acidobacteria OTUs on mud or Actinobacteria OTUs in water. Still, most of them seem to be time-dependent, which might suggest microbiota adaptation. Moreover, our CCA analysis indicated that different bacterial genera (mainly from Proteobacteria) seemed to be associated to the increase of aluminum concentration as detected in mud samples. The Betaproteobacteria family *Comamonadaceae* was detected as the most abundant in all samples. *Comamonadaceae* include psychrophilic and thermophilic species, freshwater oligotrophic, as well as heterotrophic organisms capable of denitrification and metabolization of complex organic pollutants (Zhang et al., 2013; Willems, 2014). *Comamonadaceae* species contributes to a stable consortium for sulfur-driven iron reduction combined with anaerobic ammonium oxidation via simultaneous nitrification and denitrification (Bao and Li, 2017). Once the present study does not contain samples from unimpacted areas, it is not possible to state that these *Comamonadaceae* family species are original of the microbial community before the disaster, or the wave of ore tailing transported them to the Doce River environment. However, based on a year on the time scale, it seems that this bacterial family was capable of surviving despite the high concentration of heavy metal observed in the mud. The CCA data indicated negative association (Spearman test = -0.6443; $p < 0.05$) of *Comamonadaceae* abundances with iron level and no significative correlation (Spearman test = -0.60318; $p > 0.05$) to aluminum level on samples.

*Eichhornia* presented high microbial diversity and richness in the rhizosphere. Studies have showed that *Eichhornia*, like other aquatic macrophytes, has a specialized rhizosphere microbiota capable of resisting and removing heavy metals and other water pollutants as well (Abou-Shanab et al., 2007; El-Deeb et al., 2012; Sharma et al., 2013; Kabeer et al., 2014; Irawati et al., 2017). The *Eichhornia* rhizosphere community presented the dominance of an unknown bacterial genus of *Moraxellaceae* family (17.8%), that was also observed on water samples but, interestingly, only on samples collected one year later of disaster. *Moraxellaceae* is widely distributed in nature, already been described in plants, soil, water, and sewage (Bergogne-Berezin and Towner, 1996; Teixeira and Merquior, 2014). Some *Moraxellaceae* species have shown to be resistant to heavy metals, such as Fe (Abou-Shanab et al., 2007; Akbulut et al., 2014; Jiang et al., 2017). However, a low amount of

**Table 5.** Most abundant Excavata, Fungi and SAR OTUs (relative abundance higher than 1% of the total sequences in each group) obtained by 18S rRNA amplicon sequencing. "Others" combine the OTUs with abundance lower than 1% of the sequences in each group.

| Excavata (average percentage of the total microeukaryotes = 6.14%) | Relative abundance (%) | | | | |
|---|---|---|---|---|---|
| | W13 | F13 | R13 | M1 | M13 |
| Discoba; Euglenozoa; Diplonemea; Rhynchopus | 0 | 0 | 1.42 | 0 | 0 |
| Discoba; Euglenozoa; Euglenida; Aphagea; Rhabdomonas | 3.88 | 0.01 | 0.19 | 12.05 | 24.32 |
| Discoba; Euglenozoa; Euglenida; Euglenophyceae; Euglenaceae; Euglena | 2.25 | 5.04 | 0.24 | 0 | 5.77 |
| Discoba; Euglenozoa; Euglenida; Petalomonas | 6.92 | 0.37 | 3.22 | 3.84 | 0 |
| Discoba; Euglenozoa; Kinetoplastea; Metakinetoplastina; Eubodonida; Bodo | 4.72 | 9.30 | 25.08 | 20.26 | 20.76 |
| Discoba; Euglenozoa; Kinetoplastea; Metakinetoplastina; Neobodonida OTU | 3.04 | 3.58 | 11.53 | 2.97 | 4.61 |
| Discoba; Euglenozoa; Kinetoplastea; Metakinetoplastina; Neobodonida; Neobodo | 3.22 | 77.14 | 20.54 | 21.14 | 25.50 |
| Discoba; Euglenozoa; Kinetoplastea; Metakinetoplastina; Neobodonida; Rhynchobodo | 1.48 | 0 | 3.02 | 0.70 | 0 |
| Discoba; Euglenozoa; Kinetoplastea; Metakinetoplastina; Neobodonida; Rhynchomonas | 0.05 | 3.54 | 0.59 | 3.06 | 9.43 |
| Discoba; Euglenozoa; Kinetoplastea; Metakinetoplastina; Parabodonida OTU | 0.51 | 0.33 | 0.43 | 2.18 | 0 |
| Discoba; Euglenozoa; Kinetoplastea; Metakinetoplastina; Trypanosomatida OTU | 56.69 | 0.01 | 2.61 | 0 | 0 |
| Discoba; Euglenozoa; Kinetoplastea; Prokinetoplastina; Ichthyobodo | 15.35 | 0.03 | 26.70 | 0.70 | 0 |
| Discoba; Heterolobosea; Tetramitia; Allovahlkampfia | 0 | 0.04 | 0.02 | 9.08 | 0 |
| Discoba; Heterolobosea; Tetramitia; Naegleria | 0.40 | 0.60 | 0.14 | 18.60 | 3.85 |
| Discoba; Jakobida; Andalucia | 0 | 0 | 0 | 5.07 | 0 |
| Malawimonadidae; Malawimonas | 0.23 | 0 | 0 | 0.26 | 5.77 |
| Others | 1.26 | 0.01 | 4.27 | 0.09 | 0.00 |
| Fungi (average percentage of the total microeukaryotes = 23.17%) | | | | | |
| Ascomycota | 1.40 | 0.27 | 0.70 | 0.03 | 0 |
| Ascomycota; Pezizomycotina | 1.43 | 3.23 | 1.77 | 1.29 | 1.83 |
| Ascomycota; Pezizomycotina; Dothideomycetes; Pleosporales | 0.09 | 1.21 | 0.61 | 1.07 | 0.01 |
| Ascomycota; Pezizomycotina; Dothideomycetes; Pleosporales; Phaeosphaeriaceae | 13.65 | 69.72 | 33.92 | 55.51 | 3.38 |
| Ascomycota; Pezizomycotina; Eurotiomycetes | 0.12 | 1.11 | 1.06 | 0.79 | 0.53 |
| Ascomycota; Pezizomycotina; Eurotiomycetes; Chaetothyriales | 1.07 | 0.20 | 0.92 | 0.91 | 0.38 |
| Ascomycota; Pezizomycotina; Eurotiomycetes; Chaetothyriales; Herpotrichiellaceae; Cladophialophora | 0 | 0.60 | 0.54 | 1.32 | 0.01 |
| Ascomycota; Pezizomycotina; Incertae Sedis; Incertae Sedis; Incertae Sedis; Kendrickiella | 1.94 | 2.08 | 1.75 | 1.23 | 0.35 |
| Ascomycota; Pezizomycotina; Sordariomycetes; Diaporthales; Cryphonectriaceae; Cryphonectria-Endothia complex | 0.07 | 0.09 | 0.10 | 1.71 | 0.01 |
| Ascomycota; Pezizomycotina; Sordariomycetes; Microascales | 2.08 | 0.29 | 0.72 | 0.83 | 0.34 |
| Ascomycota; Saccharomycotina; Saccharomycetes; Saccharomycetales | 3.19 | 0.32 | 0.49 | 0.18 | 0.07 |
| Ascomycota; Saccharomycotina; Saccharomycetes; Saccharomycetales; Saccharomycetaceae; Saccharomyces | 1.76 | 0.03 | 0.08 | 0.11 | 0.04 |
| Basidiomycota; Agaricomycotina | 0.51 | 0.61 | 1.24 | 0.83 | 0.02 |
| Basidiomycota; Agaricomycotina; Agaricomycetes; Agaricales | 25.37 | 4.59 | 3.78 | 1.01 | 2.78 |
| Basidiomycota; Agaricomycotina; Wallemiomycetes; Wallemiales; Incertae Sedis; Wallemia | <0.01 | 0 | 0 | 0 | 2.65 |
| Basidiomycota; Ustilaginomycotina; Malasseziomycetes; Malasseziales; Malasseziaceae; Malassezia | 8.40 | 0.04 | 0.08 | 1.87 | 1.35 |
| Basidiomycota; Ustilaginomycotina; Ustilaginomycetes; Ustilaginales; Ustilaginaceae | 0.76 | 1.47 | 3.77 | 0.13 | 0.26 |
| Blastocladiomycota; Incertae Sedis; Blastocladiomycetes; Blastocladiales | 0.01 | 0.02 | 0.34 | 10.21 | 0.06 |
| Blastocladiomycota; Incertae Sedis; Blastocladiomycetes; Blastocladiales; Blastocladiaceae | 0 | 0.02 | 1.13 | 4.37 | 0.02 |
| Chytridiomycota; Incertae Sedis; Chytridiomycetes | 2.58 | 0.49 | 7.62 | 7.49 | 3.94 |
| Chytridiomycota; Incertae Sedis; Chytridiomycetes; Chytridiales | 0 | 0 | 1.75 | 0 | 0 |
| Chytridiomycota; Incertae Sedis; Chytridiomycetes; Polychytriales; Incertae Sedis; Arkaya | 0.01 | 2.55 | 0.11 | 0.14 | <0.01 |
| Chytridiomycota; Incertae Sedis; Chytridiomycetes; Rhizophydiales | 0 | 0 | 0.23 | 1.51 | 0 |
| Chytridiomycota; Incertae Sedis; Chytridiomycetes; Spizellomycetales | 0.26 | 1.14 | 0.41 | 0.30 | 0.11 |
| Chytridiomycota; Incertae Sedis; Chytridiomycetes; Spizellomycetales; Olpidiaceae; Olpidium | 0.84 | 1.06 | 1.87 | 0.28 | 2.74 |
| Cryptomycota | 1.34 | 0.15 | 1.29 | 0.32 | 0.32 |
| Cryptomycota; LKM11 | 3.97 | 2.43 | 4.95 | 0.47 | 0.87 |
| Cryptomycota; Paramicrosporidium | 0.42 | 0.02 | 3.06 | 0 | 0.04 |
| LKM15 | 2.32 | 0.01 | 0.02 | 0 | 0 |
| Mucoromycota | 0.02 | 0.09 | 0.13 | 0 | 56.64 |
| Mucoromycota; Mucoromycotina; Mucorales; Mucoraceae | <0.01 | 0.30 | 0.69 | 1.38 | 0.10 |
| Basal Fungi | 22.05 | 3.02 | 19.15 | 2.38 | 17.71 |
| Others | 4.34 | 2.83 | 5.70 | 2.32 | 3.42 |
| SAR (average percentage of the total microeukaryotes = 50.53%) | | | | | |
| Alveolata | | | | | |
| Apicomplexa; Conoidasida; Cryptosporida; Cryptosporidium | <0.01 | <0.01 | 0.01 | 0.31 | 1.43 |
| Ciliophora; Intramacronucleata | <0.01 | 0.10 | 0.76 | 2.05 | 0.01 |
| Ciliophora; Intramacronucleata; Colpodea | 0.31 | 0.21 | 0.78 | 6.38 | 13.11 |
| Ciliophora; Intramacronucleata; Colpodea; Colpodida | 0 | 0.19 | 0 | 6.38 | 0.94 |

(*continued on next page*)

**Table 5** (*continued*)

| Excavata (average percentage of the total microeukaryotes = 6.14%) | Relative abundance (%) | | | | |
|---|---|---|---|---|---|
| | W13 | F13 | R13 | M1 | M13 |
| Ciliophora; Intramacronucleata; Litostomatea; Haptoria | 1.70 | 0.03 | 1.00 | 9.69 | 3.21 |
| Ciliophora; Intramacronucleata; Oligohymenophorea; Hymenostomatia; Tetrahymena | 0 | 0.59 | 1.74 | 0.08 | 0.32 |
| Ciliophora; Intramacronucleata; Oligohymenophorea; Peritrichia | 0.91 | 10.31 | 4.09 | 8.95 | 5.23 |
| Ciliophora; Intramacronucleata; Oligohymenophorea; Scuticociliatia | 1.23 | <0.01 | 0.96 | 0.55 | 0.01 |
| Ciliophora; Intramacronucleata; Oligohymenophorea; Scuticociliatia; Cyclidium | 1.62 | 0.01 | 0.20 | 0.58 | 0.06 |
| Ciliophora; Intramacronucleata; Phyllopharyngea; Cyrtophoria | <0.01 | 24.42 | 0.52 | 18.94 | 0.03 |
| Ciliophora; Intramacronucleata; Prostomatea | 0 | 0 | 0 | 4.49 | 0 |
| Ciliophora; Intramacronucleata; Prostomatea; Cryptocaryon | 2.12 | <0.01 | <0.01 | 0.73 | 0.06 |
| Ciliophora; Intramacronucleata; Spirotrichea | 9.31 | 0.01 | 0.02 | 0.03 | 0.01 |
| Ciliophora; Intramacronucleata; Spirotrichea; Hypotrichia | 11.01 | 0.06 | 0.73 | 4.40 | 0.63 |
| Ciliophora; Postciliodesmatophora; Heterotrichea; Blepharisma | 0.04 | 0.06 | 43.72 | 0 | 0.05 |
| Protalveolata; Perkinsidae; A31 | 17.48 | 0.03 | 0.28 | 0.94 | 0 |
| Protalveolata; Syndiniales | 2.35 | 0.09 | 0.34 | 0.32 | 0.07 |
| Rhizaria | | | | | |
| Cercozoa | 3.02 | 14.40 | 9.24 | 6.56 | 13.40 |
| Cercozoa; Cercomonadidae | 0.03 | 0.21 | 0.37 | 1.80 | 2.55 |
| Cercozoa; Clathrulinidae; Hedriocystis | 0.03 | 0.03 | 0.70 | 0.42 | 2.13 |
| Cercozoa; Glissomonadida; Heteromita | 0.17 | 3.17 | 0.75 | 3.12 | 0.38 |
| Cercozoa; Imbricatea; Silicofilosea; Euglyphida | 0.36 | 0.78 | 3.04 | 2.00 | 38.60 |
| Cercozoa; Thecofilosea; Cryomonadida; Rhizaspididae; Rhogostoma | 2.05 | 2.98 | 2.91 | 0.69 | 5.64 |
| Cercozoa; Vampyrellidae | 0.03 | 0 | 1.10 | 0 | 0.52 |
| Stramenopiles | | | | | |
| Bicosoecida | 2.82 | <0.01 | 0.74 | 1.86 | 0.05 |
| Bicosoecida; Bicosoeca | 5.88 | 0.24 | 0.27 | 0.94 | 0.01 |
| Labyrinthulomycetes; Amphitraemidae | 0.31 | 0.03 | 1.12 | 0.08 | 0.45 |
| Labyrinthulomycetes; Sorodiplophrys | 2.63 | 0.48 | 3.75 | 0.41 | 0.01 |
| Ochrophyta | 0.84 | 0.36 | 0.16 | 0.55 | 3.21 |
| Ochrophyta; Chrysophyceae | 10.76 | 18.96 | 7.09 | 3.38 | 0.53 |
| Ochrophyta; Chrysophyceae; Chromulinales | 6.81 | 16.97 | 5.97 | 3.71 | 0.45 |
| Ochrophyta; Chrysophyceae; Ochromonadales; Paraphysomonas | 7.36 | 0.52 | 1.99 | 0.50 | 0.14 |
| Ochrophyta; Chrysophyceae; P34.45 | 2.03 | 0.26 | 0.43 | 1.53 | 0.05 |
| Peronosporomycetes; Phytophthora | 0.97 | 1.13 | 0.78 | 1.46 | 0.98 |
| Others | 5.81 | 3.36 | 4.43 | 6.17 | 5.71 |

*Moraxella* was observed on mud samples, place where a relevant number of heavy metals were detected in high concentration. The Spearman rank test indicates a negative association of *Moraxellaceae* OTU to aluminum concentration on samples (Spearman test = -0.7060; $p < 0.05$).

Analyses of microeukaryotic communities revealed a diverse composition of taxa in all samples, including different groups of Fungi, SAR, Excavata and Amoebozoa. Each one of these groups were characterized by dominance. More than 80 OTUs were identified in Fungi group, and their overall distribution through samples did not demonstrated any profile of microenvironment dependence. Differently in Excavata, an OTU belonging to the family *Trypanosomatida* was identified in abundance in water samples but was not observed on mud samples. This family deserves special attention since it includes genera as *Trypanosoma* that represent a significant public health threat in Brazil (Lidani et al., 2019). In contrast, *Neobodonida* (genus *Neobodo*) was identified in water samples but was highly abundant in mud samples. The acidity of water (pH 6.3) and the heavy metals concentration (Table 2) on mud might be responsible to the microorganism's selectivity. However, future studies with large sampling would confirm this supposition.

Microenvironment differences in microbiota modulation were more evident on the supergroup Amoebozoa. They are a highly diverse group of phagotrophic protists that includes species characterized as free-living amoeba (FLA) (Saburi et al., 2017). The life forms of these microorganisms include cysts (Sriram et al., 2008), which are resistance forms that favor dispersion and its perpetuation in singular environments. Although FLAs are widespread in freshwater ecosystems, their relative abundance is low, with no more than 5%–10% of total protists in reservoirs and rivers (Ren et al., 2018).

At the genus level, we detected *Acanthamoeba* as the most frequent within Amoebozoa, which interestingly occurred in high abundances in mud samples that presented high concentrations of metals. *Acanthamoeba* is a type of small, naked and free-living amoebae genus that occurs in most habitats such as in soil, air, dust, and water. In their natural environment, these organisms feed on bacteria and particulate matters. Most of these studies report this genus as a risk to human health when its species are occurring in water bodies and drinking water (Sente et al., 2016; Armand et al., 2016; Fallah et al., 2017; Spotin et al., 2017; Xuan et al., 2017; Basher et al., 2018). *Acanthamoeba* is described as the most common FLA genus in different aquatic environments (Magnet et al., 2013) and its prevalence is dependent on the water temperature and turbidity (Ren et al., 2018). Few data reported the metal tolerance of *Acanthamoeba*. A study that investigated the IC50 value of Mn in relation to an *Acanthamoeba* sp. environmental isolate indicated that 24 h exposure of this metal induced apoptotic and necrotic cell death, as well as mild genotoxicity towards DNA (Hashim et al., 2015). Our data from CCA analysis indicated a high abundance of amoeba OTUs, including the genus *Acanthamoeba,* as likely to be found where iron concentration is increased. Moreover, we isolated *Acanthamoeba* from a mud sample (that presented increased levels of different heavy metals), which was confirmed by 18S rRNA gene fragment sequencing as a member of *Acanthamoeba lenticulata.* All these data indicate that this genus may at least tolerate the toxic environmental condition imposed on the Doce

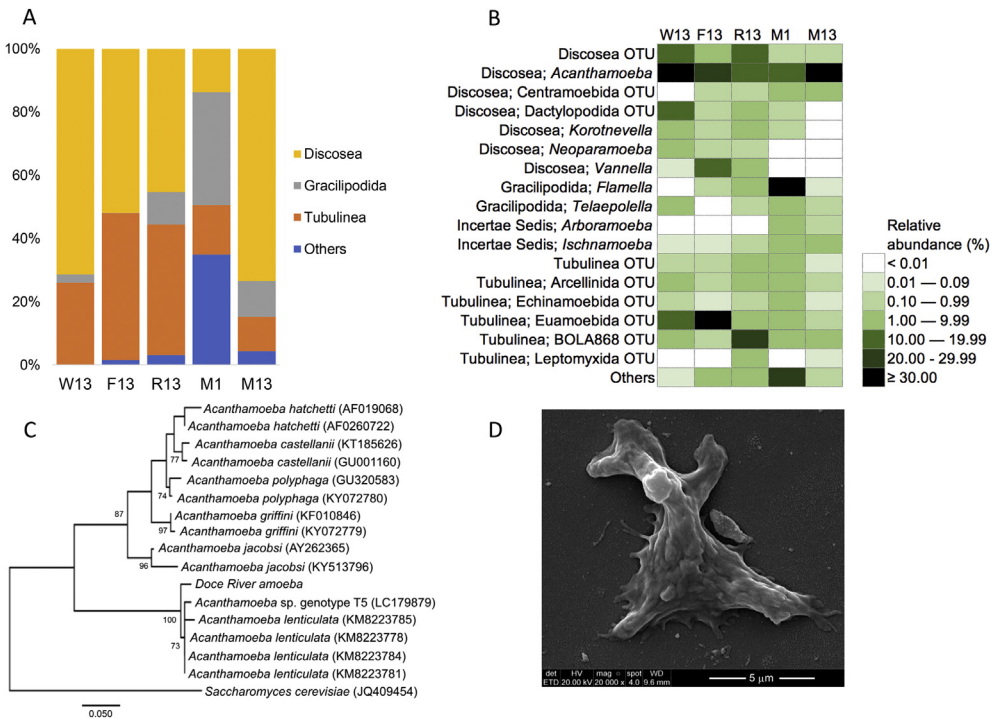


**Figure 6.** Identification of the amoebozoans from the Doce River. (A) most abundant amoebozoan groups; and (B) genera or corresponding OTUs identified by 18S rRNA amplicon sequencing; (C) phylogenetic analysis of the isolate "Doce River amoeba" based on a 400 bp-long fragment of the 18S rRNA partial gene sequencing. Amoeba DNA sequences from the same 18S rRNA gene (region V3) were retrieved from GenBank. Values above branches indicate the bootstrap support; (D) SEM image of the amoeba from the same culture used to the molecular characterization.

River. Like other species of *Acanthamoeba, A. lenticulata* have been isolated from or detected in different environmental samples in previous studies (Sente et al., 2016; Fallah et al., 2017; Spotin et al., 2017; Xuan et al., 2017; Basher et al., 2018). However, this work seems to be the first report of isolation if this amoeba species from a profoundly impacted environment.

First reported as in high concentration in the Doce River mud (Carvalho et al., 2017, 2018), iron ions are required in many biological processes as metalloprotein components and enzyme cofactors in most microorganisms. However, they may behave as toxic compounds at high concentrations (Bruins et al., 2000; Porcheron et al., 2013). Among the bacterial isolates obtained from sample M1, few bacteria survived under the lowest concentration of iron tested in our culture media. However, three microbiological isolates were tolerant to high iron concentration (1 mM). The study by Collins-Fairclough et al. (2018), based on metagenome data, detected bacterial pathogens that had extensive predictive profiles of distinct metal resistance at Jamaica's largest solid waste disposal site and an anthropogenically impacted river. Possibly many other bacterial isolates could have been obtained since our cultures were based on the limitation of few culturing media. Future studies to identify and characterize isolates will determine the importance of those isolates in a heavy metal environment microbiome.

The evident calamitous, poisoning, severe impact of the 'wave of mud' on Doce River (Creado and Helmreich, 2018) was carried across over 660 km in two weeks until it reached in the Atlantic Ocean. In this context, the information about the microbiota that resisted the hostile environment in the Doce River basin might give us insights regards the consequences of long-term anthropogenic impacts on aquatic

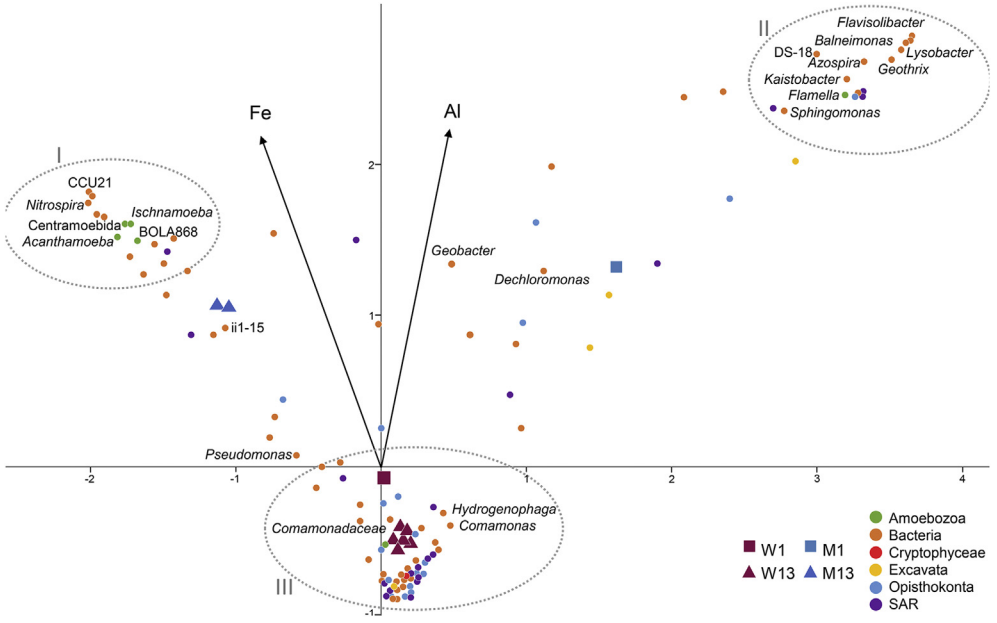


**Figure 7.** Correlation of metal concentration with the microbial communities. Canonical correlation analysis (CCA) triplot with symmetrical scaling indicating differences in iron and aluminum concentrations within water and mud samples, and influence of these abiotic variables on the prokaryotic and microeukaryotic individual taxa. W = water samples; M = mud samples. OTUs were pointed out as follows: green dot = Amoebozoa; orange dot = Bacteria; red dot = Cryptophyceae; yellow dot = Excavata; blue dot = Opisthokonta; purple dot = SAR.

ecosystems, as well as strategies for the recovery of contaminated sites. The detection of metal tolerant microbiota in the Doce River water, mud, foam, and *Eichhornia* rhizosphere can be explained as a result of the selection by the long-term presence of high concentrations of metals in the river since the first moments after the disaster. Continuous research on the characterization of microbial isolates obtained in the present study should elucidate mechanisms to be explored for some future bioremediation strategies in highly impacted environments, such as the Doce River.

## 5. Conclusion

Samples of water, mud, foam, and rhizosphere of *Eichhornia* from Doce River were collected one month and thirteen months after the collapse of two ore tailing dams in November 2015. They were analyzed through 16S and 18S rRNA-based amplicon sequencing and microbial isolation, chemical, and mineralogical analyses. Our data indicated that microbial groups containing metal tolerant taxa were detected in high frequencies in all samples. The prokaryotic communities from mud samples shifted drastically over time, whereas a higher similarity was found between water samples in the same period. A reduction in the diversity of microeukaryotes was observed, with a parallel increase in Amoebozoans abundance. Also, an isolate of *Acanthamoeba lenticulata* was obtained, which may represent the first report of isolation if this species from a highly impacted environment.

Moreover, the isolated bacteria were tolerant to high concentrations of the metals tested. Based on these data, especially on the change in microbial communities' structure, we concluded that the microbiome from Doce River might have adapted to the long-term exposure to high concentrations of heavy metals of this highly contaminated environment. Our data thus indicated that the characterization of microbial communities and metal-tolerant organisms from impacted environments, like the Doce River, is essential for understanding the ecological consequences of massive anthropogenic damages, and strategies for restoration of such disturbed sites.

## Declarations

### *Author contribution statement*

Adriana Giongo, João Marcelo Medina Ketzer, Renata Medina-Silva: Conceived and designed the experiments; Analyzed and interpreted the data; Wrote the paper.

Luiz Gustavo dos Anjos Borges, Maria Pilar Serbent, Rosalia Barili: Analyzed and interpreted the data; Wrote the paper.

Letícia Marconatto, Pâmela de Lara Palhano, Lisiê Valéria Paz, Letícia Isabela Moser: Performed the experiments.

Eduardo Moreira-Silva: Analyzed and interpreted the data.

Tiago de Abreu Siqueira: Analyzed and interpreted the data; Contributed reagents, materials, analysis tools or data.

Caroline Thais Martinho: Performed the experiments; Analyzed and interpreted the data; Contributed reagents, materials, analysis tools or data.

Carolina De Marco Veríssimo: Performed the experiments; Contributed reagents, materials, analysis tools or data.

### *Funding statement*

This work was supported by IPR/PUCRS Research Funding. Funding was also provided in part by the CNPq (Brazilian National Council for Scientific and Technological Development); (scholarships for master's degree); and CAPES (Coordination for the Improvement of Higher Education Personnel; finance code 001).

### *Competing interest statement*

The authors declare no conflict of interest.

### *Additional information*

No additional information is available for this paper.

## Acknowledgements

We thank Guga Ketzer and Jon Rose from the non-profit organization "Waves for Water" (http://www.wavesforwater.org) for the sampling effort in 2015, Luiz F. Rodrigues for his advice in technical issues in the original project, Adolpho H. Augustin for the map preparation and Fernanda de Jesus Trindade and Eduardo Eizirik for helping about the phylogenetic analysis. Luiz Gustavo dos A. Borges thanks PEGA/PUCRS. We also thank the High-Performance Computing Lab (LAD/PUCRS) for allowing access to run the high-throughput computational analyses; the Central Laboratory of Microscopy and Microanalysis (LabCEMM/PUCRS) for preparing and assisting the microscopic visualization. We thank the two Brazilian funding agencies, CNPq (Brazilian National Council for Scientific and Technological Development) and CAPES (Coordination for the Improvement of Higher Education Personnel), for scholarships for master's degree.

## References

Abou-Shanab, R.A.I., Angle, J.S., Van Berkum, P., 2007. Chromate-tolerant bacteria for enhanced metal uptake by *Eichhornia crassipes* (Mart.). Int. J. Phytoremediation 9, 91–105.

Adl, S.M., Simpson, A.G.B., Lane, C.E., Lukes, J., Bass, D., et al., 2012. Revision classification of eukaryotes. J. Eukaryot. Microbiol. 59, 429–493.

Adl, S.M., Bass, D., Lane, C.E., Lukes, J., Schock, C.L., et al., 2019. Revision of the classification, nomenclature and diversity of eukaryotes. J. Eukaryot. Microbiol. 66, 4–119.

Akbulut, S., Yilmaz, F., Icgen, B., 2014. Surface water isolates of hemolytic and non-hemolytic *Acinetobacter* with multiple drug and heavy metal resistance ability. J. Water Health 12, 1–12.

Amin, N.M., 2012. "Techniques for assessment of heavy metal toxicity using *Acanthamoeba* sp., a small, naked and free-living amoeba". In: Ali, Mahamane (Ed.), The Functioning of Ecosystems, pp. 200–212.

Armand, B., Motazedian, M.H., Asgari, Q., 2016. Isolation and identification of pathogenic free-living amoeba from surface and tap water of Shiraz City using morphological and molecular methods. Parasitol. Res. 115, 63–68.

ASTM, 2000. (2000) Standard Test Method for Turbidity of Water (Withdrawn 2007); D1889–00. ASTM International, West Conshohocken, PA. Available online. www.astm.org (accessed on 01 May 2020).

ASTM, 2019. Standard Test Method for pH of Aqueous Solutions with the Glass Electrode; ASTM E70–19. ASTM International, West Conshohocken, PA. Available online. www.astm.org (accessed on 01 May 2020).

Azarbad, H., van Gestel, C.A.M., Niklinska, M., Laskowski, R., Röling, W.F.M., van Straalen, N.M., 2016. Resilience of soil microbial communities to metals and additional stressors: DNA-based approaches for assessing "stress-on-stress" responses. Int. J. Mol. Sci. 17, 933.

Bao, P., Li, G.X., 2017. Sulfur-driven iron reduction coupled to anaerobic ammonium oxidation. Environ. Sci. Technol. 51, 6691–6698.

Basher, M.H.A., Ithoi, I., Mahmud, R., Abdulsalam, A.M., Foead, A.I., Dawaki, S., et al., 2018. Occurrence of *Acanthamoeba* genotypes in central west Malaysian environments. Acta Trop. 178, 219–228.

Bates, S.T., Berg-Lyons, D., Caporaso, J.G., Walters, W.A., Knight, R., Fierer, N., 2011. Examining the global distribution of dominant archaeal populations in soil. ISME J. 5, 908–917.

Bergogne-Berezin, E., Towner, K.J., 1996. *Acinetobacter* spp. as nosocomial pathogens: microbiological, clinical, and epidemiological features. Clin. Microbiol. Rev. 9, 148–165.

Bruins, M.R., Kapil, S., Oehme, F.W., 2000. Microbial resistance to metals in the environment. Ecotoxicol. Environ. Saf. 45, 198–207.

Caporaso, J.G., Kuczynski, J., Stombaugh, J., Bittinger, K., Bushman, F.D., Costello, E.K., et al., 2010. QIIME allows analysis of high-throughput community sequencing data. Nat. Methods 7, 335–336.

Carmo, F.F., Kamino, L.H.Y., Junior, R.T., de Campos, I.C., Carmo, F.F., Silvino, G., et al., 2017. Fundão tailings dam failures: the environment tragedy of the largest technological disaster of Brazilian mining in global context. Persp. Ecol. Cons. 15, 145–151.

Carvalho, M.S., Ribeiro, K.D., Moreira, R.M., de Almeida, A.M., 2017. Concentração de metais no Rio Doce em Mariana, Minas Gerais, Brasil. Acta Brasil. 1, 37–41.
Carvalho, G.O., Pinheiro, A.A., Sousa, D.M., Padilha, J.A., Souza, J.S., Galvão, P.M., Paiva, T.C., Freire, A.S., Santelli, R.E., Malm, O., Torres, J.P.M., 2018. Metals and arsenic in water supply for riverine communities affected by the largest environmental disaster in Brazil: the dam collapse on Doce River. Orbital - Electron. J. Chem. 10, 299–307.
Chen, Y., Jiang, Y., Huang, H., Mou, L., Ru, J., Zhao, J., Xiao, S., 2018. Long-term and high-concentration heavy-metal contamination strongly influences the microbiome and functional genes in Yellow River sediments. Sci. Total Environ. 637, 1400–1412.
Cole, J.R., Wang, Q., Fish, J.A., Chai, B., McGarrell, D.M., Sun, Y., et al., 2013. Ribosomal Database Project: data and tools for high throughput rRNA analysis. Nucleic Acids Res. 42, 633–642.
Collins-Fairclough, A.M., Ellis, M.C., Hug, L.A., 2018. Widespread antibiotic, biocide, and metal resistance in microbial communities inhabiting a municipal waste environment and anthropogenically impacted river. mSphere 3, 18–346.
CONAMA, 2005. Conselho Nacional Do Meio Ambiente. Resolução Nº 357, 17th March, 2005, Brazil.
Creado, E.S.J., Helmreich, S., 2018. A wave of mud: the travel of toxic water, from Bento Rodrigues to the Brazilian Atlantic. Revista do Instituto de Estudos Brasileiros 69, 33–51.
Eaton D, Andrew, Clesceri S, Lenore, Greenberg E, Arnold, Franson, 1998. Standard methods for the examination of water and wastewater. American Public Health Association, Washington, DC.
El-Deeb, B., Gherbawy, Y., Hassan, S., 2012. Molecular characterization of endophytic bacteria from metal hyperaccumulator aquatic plant (*Eichhornia crassipes*) and its role in heavy metal removal. Geomicrobiol. J. 29, 906–915.
EPA, 2007. EPA's 2007 Report on the Environment: Science Report. U.S. Environmental Protection Agency, Office of Research and Development. Washington, DC.
Escobar, H., 2015. Mud tsunami wreaks ecological havoc in Brazil. Science 350, 1138–1139.
Fallah, E., Jafarpour, Z., Mahami-Oskouei, M., Haghighi, A., Niyyati, M., Spotin, A., et al., 2017. Molecular characterization of *Acanthamoeba* isolates from surface resting waters in Northwest Iran. Iran. J. Parasitol. 12, 355–363.
Fernandes, G.W., Goulart, F.F., Ranieri, B.D., Coelho, M.S., Dales, K., Boesche, N., et al., 2016. Deep into the mud: ecological and socio-economic impacts of the dam breach in Mariana, Brazil. Braz. J. Nat. Cons. (Natureza & Conservação) 14, 35–45.
Garris, H.W., Baldwin, S.A., Taylor, J., Gurr, D.B., Denesiuk, D.R., Van Hamme, J.D., et al., 2018. Short-term microbial effects of a large-scale mine-tailing storage facility collapse on the local natural environment. PLoS One 13 (4), e0196032.
Giovanella, P., Cabral, L., Bento, F.M., Gianello, C., Camargo, F.A.O., 2016. Mercury (II) removal by resistant bacterial isolates and mercuric (II) reductase activity in a new strain of *Pseudomonas* sp. B50A. N. Biotech. 33, 216–223.
Giovanella, P., Cabral, L., Costa, A.P., de Oliveira Camargo, F.A., Gianello, C., Bento, F.M., 2017. Metal resistance mechanisms in Gram-negative bacteria and their potential to remove Hg in the presence of other metals. Ecotoxicol. Environ. Saf. 140, 162–169.
Gomes, L.C., Chippari-Gomes, A.R., Miranda, T.O., Pereira, T.M., Merçon, J., Davel, V., et al., 2018. Genotoxicity effects on *Geophagus brasiliensis* fish exposed to Doce River water after the environmental disaster in the city of Mariana, MG, Brazil. Braz. J. Biol. 79, 659–664.
Guerra, M.B.B., Teaney, B.T., Mount, B.J., Asunskis, D.J., Jordan, B.T., Barker, R.J., Santos, E.E., Schaefer, C.E.G.R., 2017. Post-catastrophe analysis of the fundão tailings dam failure in the Doce River system, southeast Brazil: potentially toxic elements in affected soils. Water Air Soil Pollut. 228, 252.
Hammer, O., Harper, D.A.T., Ryan, P.D., 2001. PAST: paleontological statistics software package for education and data analysis. Palaeontol. Electron. 4, 9. Available at. http://palaeo-electronica.org/2001_1/past/issue1_01.htm.
Hashim, F., Rahman, N.A.A., Amin, N.M., 2015. Morphological analysis on the toxic effect of manganese on *Acanthamoeba* sp. isolated from Setiu Wetland, Terengganu: an in vitro study. Proc. Environ. Sci. 30, 15–20.
Hatam, I., Petticrew, E.L., French, T.D., Owens, P.N., Laval, B., Baldwin, S.A., 2019. The bacterial community of Quesnel Lake sediments impacted by a catastrophic mine tailing spill differ in composition from those at undisturbed location – two years post-spill. Sci. Rep. 9, 2705.
Hatje, V., Pedreira, R.M., de Rezende, C.E., Schettini, C.A.F., de Souza, G.C., Marin, D.C., et al., 2017. The environmental impacts of one of the largest tailing dam failures worldwide. Sci. Rep. 7, 10706.
Hem, J.D., Cropper, W.H., 1959. Survey of ferrous-ferric chemical equilibria and redox potentials. USGPO 1459, 31.
Hu, X., 2014. Ciliates in extreme environments. J. Eukaryot. Microbiol. 61, 410–418.
IBAMA, 2015. Diretoria de Proteção Ambiental. Coordenação Geral de Emergências Ambientais. Laudo Técnico Preliminar: Impactos ambientais decorrentes do desastre envolvendo o rompimento da barragem de Fundão, em Mariana, Minas Gerais. Instituto Brasileiro do Meio Ambiente e dos Recursos Naturais Renováveis (IBAMA), Brasília, Brazil.
Irawati, W., Parhusip, A.J.N., Sopiah, N., Tnunay, J.A., 2017. The role of heavy metals-resistant bacteria *Acinetobacter* sp. in copper phytoremediation using *Eichhornia crasippes* [(Mart.) Solms]. In: NRLS Conference Proceedings, International Conference on Natural Resources and Life Sciences, 3, pp. 208–220.
Jiang, J., Pan, C., Xiao, A., Yang, X., Zhang, G., 2017. Isolation, identification, and environmental adaptability of heavy-metal-resistant bacteria from ramie rhizosphere soil around mine refinery. 3 Biotech 7, 5.
Kabeer, R., Varghese, R., Kochu, J.K., George, J., Sasi, P.C., Poulose, S.V., 2014. Removal of copper by *Eichhornia crassipes* and the characterization of associated bacteria of the rhizosphere system. Environ. Asia 7, 19–29.
Khan, N.A., Jarroll, E.L., Paget, T.A., 2001. *Acanthamoeba* can be differentiated by the polymerase chain reaction and simple plating assays. Curr. Microbiol. 43, 204–208.
Kumar, S., Stecher, G., Li, M., Knyaz, C., Tamura, K., 2018. MEGA X: molecular evolutionary genetics analysis across computing platforms. Mol. Biol. Evol. 35, 1547–1549.
Lidani, K.C.F., Andrade, F.A., Bavia, L., Damasceno, F.S., Beltrame, M.H., Messias-Reason, I.J., Sandri, T.L., 2019. Chagas disease: from discovery to a worldwide health problem. Front. Publ. Health 7, 166.
Liu, Q.M., Ten, L.N., Im, W.T., Lee, S.T., 2008. *Castellaniella caeni* sp. nov., a denitrifying bacterium isolated from sludge of a leachate treatment plant. Int. J. Syst. Evol. Microbiol. 58, 2141–2146.
Magnet, A., Fenoy, S., Galvan, A.L., Izquierdo, F., Rueda, C., Fernandez Vadillo, C., del Aguila, C., 2013. A year long study of the presence of free-living amoeba in Spain. Water Res. 47, 6966–6972.
McMurdie, J.P., Holmes, S., 2013. phyloseq: an R package for reproducible interactive analysis and graphics of microbiome census data. PloS One 8 (4), e61217.
Miranda, L.S., Marques, A.C., 2016. Hidden impacts of the Samarco mining waste dam collapse to Brazilian marine fauna - an example from the staurozoans (Cnidaria). Biota Neotropica 16, 2.
Neves, A.C.O., Nunes, F.P., de Carvalho, F.A., Fernandes, G.W., 2016. Neglect of ecosystems services by mining, and the worst environmental disaster in Brazil. Natureza & Conservação 1, 24–27.
Nolte, V., Pandey, R.V., Jost, S., Medinger, R., Ottenwaelder, B., Boenigk, J., et al., 2010. Contrasting seasonal niche separation between rare and abundant taxa conceals the extent of protist diversity. Mol. Ecol. 19, 2908–2915.
Perales-Vela, H.V., Peña-Castro, J.M., Cañizares-Villanueva, R.O., 2006. Heavy metal detoxification in eukaryotic microalgae. Chemosphere 64, 1–10.
Piotrowska-Seget, Z., Cycon, M., Kozdroj, J., 2005. Metal-tolerant bacteria occurring in heavily polluted soil and mine spoil. Appl. Soil Ecol. 28, 237–246.
Płachno, B.J., Wołowski, K., Augustynowicz, J., Łukaszek, M., 2015. Diversity of algae in a thallium and other heavy metals-polluted environment. Ann. Limnol. Int. J. Limnol. 51, 139–146.
Pobi, K.K., Satpati, S., Dutta, S., Nayek, S., Saha, R.N., Gupta, S., 2019. Sources evaluation and ecological risk assessment of heavy metals accumulated within a natural stream of Durgapur industrial zone, India, by using multivariate analysis and pollution indices. Appl. Water Sci. 9, 58.
Porcheron, G., Garénaux, A., Proulx, J., Sabri, M., Dozois, C.M., 2013. Iron, copper, zinc, and manganese transport and regulation in pathogenic Enterobacteria: correlations between strains, site of infection and the relative importance of the different metal transport systems for virulence. Front. Cell. Infect. Microbiol. 3, 90.
Quadra, G.R., Roland, F., Barros, N., Malm, O., Lino, A.S., Azevedo, G.M., et al., 2019. Far-reaching cytogenotoxic effects of mine waste from the Fundão dam disaster in Brazil. Chemosphere 215, 753–757.
Quast, C., Pruesse, E., Yilmaz, P., Gerken, J., Schweer, T., Yarza, P., et al., 2013. The SILVA ribosomal RNA gene database project: improved data processing and web-based tools. Nucleic Acids Res. 41, 590–596.
Queiroz, H.M., Nóbrega, G.N., Ferreira, T.O., Almeida, L.S., Romero, T.B., Santaella, S.T., et al., 2018. The Samarco mine tailing disaster: a possible time-bomb for heavy metals contamination? Sci. Total Environ. 637, 498–506.
Rehman, A., 2011. Heavy metals uptake by *Euglena proxima* isolated from tannery effluents and its potential use in wastewater treatment. Russ. J. Ecol. 42, 44–49.
Ren, K., Xue, Y., Rønn, R., Liu, L., Chen, H., Rensing, C., Yang, J., 2018. Dynamics and determinants of amoeba community, occurrence and abundance in subtropical reservoirs and rivers. Water Res. 146, 177–186.
Rinke, C., Schwientek, P., Sczyrba, A., Ivanova, N.N., Anderson, I.J., Cheng, J.-F., Darling, A., Malfatti, S., Swan, B.K., Gies, E.A., Dodsworth, J.A., Hedlund, B.P., Tsiamis, G., Sievert, S.M., Liu, W.-T., Eisen, J.A., Hallam, S.J., Kyrpides, N.C., Stepanauskas, R., Rubin, E.M., Hugenholtz, P., Woyke, T., 2013. Insights into the phylogeny and coding potential of microbial dark matter. Nature 499, 431–437.
SAAE, 2015. Relatório analítico parcial. Serviço Autotnomo de Água e Esgoto de Minas Gerais, Brazil.
Saburi, E., Rajaii, T., Behdari, A., Kohansal, M.H., Vazini, H., 2017. Free-living amoebae in the water resources of Iran: a systematic review. J. Parasit. Dis. 41, 919–928.
Savio, D., Sinclair, L., Ijaz, U.Z., Parajka, J., Reischer, G.H., Stadler, P., Blaschke, A.P., Blöschl, G., Mach, R.L., Kirschner, A.K.T., Farnleitner, A.H., Eiler, A., 2015. Bacterial diversity along a 2600 km river continuum. Environ. Microbiol. 17, 4994–5007.
Schroeder, J.M., Booton, G.C., Hay, J., Niszl, I.A., Seal, D.V., Markus, M.B., et al., 2001. Use of subgenic 18S ribosomal DNA PCR and sequencing for genus and genotype identification of acanthamoebae from humans with keratitis and from sewage sludge. J. Clin. Microbiol. 39, 1903–1911.
SEDRU, 2016. Avaliacão dos efeitos e desdobramentos do rompimento da Barragem de Fundão em Mariana-MG. Secretaria de Estado de Desenvolvimento Regional, Política Urbana e Gestão Metropolitana (SEDRU), Belo Horizonte, Brazil.
Segura, F.R., Nunes, E.A., Paniz, F.P., Paulelli, A.C.C., Rodrigues, G.B., Braga, G.Ú.L., et al., 2016. Potential risks of the residue from Samarco's mine dam burst (Bento Rodrigues, Brazil). Environ. Pollut. 218, 813–825.
Sente, C., Erume, J., Naigaga, I., Magambo, P.K., Ochwo, S., Mulindwa, J., et al., 2016. Occurrence and genetic characterisation of *Acanthamoeba* spp. from environmental and domestic water sources in Queen Elizabeth Protected Area, Uganda. Parasites Vectors 9, 127.
Sharma, R., Sharma, K., Singh, N., Kumar, A., 2013. Rhizosphere biology of aquatic microbes in order to access their bioremediation potential along with different aquatic macrophytes. Recent Res. Sci. Technol. 5, 29–32.
Silva, G.P., Fontes, M.P.F., da Costa, L.M., de Barros, N.F., 2006. Caracterização química, física e mineralógica de estéreis e rejeito da mineração de ferro da Mina de Alegria, Mariana-MG. Pesqui. Agropecuária Trop. 36, 45–52.

Silva, A.C., Cavalcante, L.C.D., Fabris, J.D., Franco Júnior, R., Barral, U.M., de Melo Farnezi, M.M., Viana, A.J.S., Ardisson, J.D., Fernandez-Outon, L.E., Lara, L.R.S., Stumpf, H.O., Barbosa, J.B.S., Silva, L.C., 2017. Chemical, mineralogical and physical characteristics of a material accumulated on the river margin from mud flowing from the collapse of the iron ore tailings dam in Bento Rodrigues, Minas Gerais, Brazil. Revista Espinhaço 5 (2), 44–53.

SOS Mata Atlântica, INPE, 2016. Análise do impacto sobre áreas de Mata Atlântica do rompimento da barragem localizada no subdistrito de Bento Rodrigues, no município de Mariana – MG. SOS Mata Atlântica e Instituto Nacional de Pesquisas Espaciais (INPE), Brasília.

Spotin, A., Moslemzadeh, H.R., Mahami-Oskouei, M., Ahmadpour, E., Niyyati, M., Hejazi, S.H., et al., 2017. Phylogeography, genetic variability and structure of *Acanthamoeba* metapopulations in Iran inferred by 18S ribosomal RNA sequences: a systematic review and meta-analysis. Asian Pac. J. Trop. Med. 10, 855–863.

Sriram, R., Shoff, M., Booton, G., Fuerst, P., Visvesvara, G.S., 2008. Survival of *Acanthamoeba* cysts after desiccation for more than 20 years. J. Clin. Microbiol. 46, 4045–4048.

Tamura, K., Nei, M., 1993. Estimation of the number of nucleotide substitutions in the control region of mitochondrial DNA in humans and chimpanzees. Mol. Biol. Evol. 10, 512–526.

Teixeira, L.M., Merquior, V.L.C., 2014. "The family Moraxellaceae" in the prokaryotes: gammaproteobacteria. In: Rosenberg, E., DeLong, E.F., Lory, S., Stackebrandt, E., Thompson, F. (Eds.). Springer, Berlin: Heidelberg, pp. 443–476.

Torres, J.P.M., Spuza, J., Padilha, J., Oliveira, G., Paiva, T., 2017. Contaminação por metais pesados na água utilizada por agricultores familiares na Região do Rio Doce. Relatório Greenpeace 1–37.

Van der Gucht, K., Vandekerckhove, T., Vloemans, N., Cousin, S., Muylaert, K., Sabbe, K., Gillis, M., Declerk, S., De Meester, L., Vyverman, W., 2005. Characterization of bacterial communities in four freshwater lakes differing in nutrient load and food web structure. FEMS (Fed. Eur. Microbiol. Soc.) Microbiol. Ecol. 53, 205–220.

Vieira, C.K., dos Anjos Borges, L.G., Marconatto, L., Giongo, A., Stürmer, S.L., 2018. Microbiome of a revegetated iron-mining site and pristine ecosystems from the Brazilian Cerrado. Appl. Soil Ecol. 131, 55–65.

Visvesvara, G.S., 1991. Classification of Acanthamoeba. Rev. Infect. Dis. 13, S369–372.

Willems, A., 2014. In: Rosenberg, E., DeLong, E.F., Lory, S., Stackebrandt, E., Thompson, F. (Eds.), "The family Comamonadaceae" in the prokaryotes: alphaproteobacteria and betaproteobacteria. Springer, Berlin: Heidelberg, pp. 777–851.

Xia, N., Xia, X., Liu, T., Hu, L., Zhu, B., Zhang, X., Dong, J., 2014. Characteristics of bacterial community in the water and surface sediment of the Yellow River, China, the largest turbid river in the world. J. Soils Sediments 14, 1894–1904.

Xuan, Y., Shen, Y., Ge, Y., Yan, G., Zheng, S., 2017. Isolation and identification of *Acanthamoeba* strains from soil and tap water in Yanji, China. Environ. Health Prev. Med. 22, 58.

Yuan, G., Theng, B., Churchman, J., Gates, W., 2013. Clays and clay minerals for pollution control. In: Developments in clay Science, pp. 587–644.

Zettler, L.A.A., Gómez, F., Zettler, E., Keenan, B.G., Amils, R., Sogin, M.L., 2002. Eukaryotic diversity in Spain's river of fire. Nature 417, 137.

Zhang, J., Wang, Y., Zhou, S., Wu, C., He, J., Li, F., 2013. *Comamonas guangdongensis* sp. nov., isolated from subterranean forest sediment, and emended description of the genus *Comamonas*. Int. J. Syst. Evol. Microbiol. 63, 809–814.